Setting up a system to study the role of substrate stiffness on neural crest Epithelial to Mesenchymal Transition (EMT)

John Qi
UCL
MPhil Developmental and Stem Cell Biology

Table of Contents

Declaration 4

Abstract 5

Impact statement 7

Acknowledgements 9

List of tables and Figures 10

List of Figures 10

List of tables: 10

List of Abbreviations 11

Chapter 1: Introduction 13

Stem cells and early development 13

Neural crest cells 16

Epithelial-to-Mesenchymal Transition (EMT) 21

Mechanobiology 27

Significance of NCC 32

Creating a system to study the role of stiffness on EMT 34

Aims 39

Chapter 2: Materials and methods 40

Fibronectin/Matrigel coated plates 41

hiPSC and NBC thawing and maintenance 41

Cell Passaging 42

Cell cryopreservation 42

Differentiation of human induced pluripotent stem cells (iPSC) to NBC 42

Differentiation of NBC to NCC 43

Gel protocol 44

Immunostaining: 44

Real-time quantitative PCR 45

Atomic Force Microscopy (AFM) 46

Immunofluorescence and time-lapse imaging: 47

Time-lapse imaging: 47

Data Analysis: 47

Chapter 3: Results 49

Protocol of Neural crest induction of hiPSC 49

Culturing cells on substates of different stiffness: a morphological and cell behaviour analysis 55

Culturing cells on substates of different stiffness: a molecular analysis 65

Chapter 4: Summary and Discussion 71

Summary 71

Discussion 72

References: 81

Declaration

I declare that all work submitted in this document is my own work and does not involve plagiarism of any kind. Any external research mentioned has been cited for in the references section of this document. All research mentioned has been conducted by my own hands and through my own involvement.

Abstract

The neural crest is a highly migratory embryonic cell population known to differentiate into a multitude of various cell types such as the neurons, bone and pigment cells (Theveneau & Mayor, 2012), among many others. However, this diversity also requires them to migrate to various regions of the organism, leading to proper function. To do so, they must undergo a process known as Epithelial to Mesenchymal Transition (EMT). In the epithelial state, cell often adhere to neighbouring cells, maintaining an apical-basal cell polarity, and lacking cell motility. Yet, as they undergo EMT they become more migratory losing their cell-cell adhesion and apical-basal cell polarity.

Although neural crest cell (NCC) EMT is widely studied and various genes and transcription factors have been identified, the process is still not completely understood. One factor that has recently been suggested to influence EMT is the mechanical properties of the substrate. A recent paper by Barriga et al. indicates that EMT can be inhibited by softening the underlying stiffness. To study the mechanism that is controlling EMT through stiffness, a robust and reproducible system needs to be developed. In this project, we aim to develop a system to study the role of how the substrate stiffness affects EMT of NCC in human cells *in vitro*. To do this, the precursors of NCCs, called neural border cells (NBC), are plated on polyacrylamide gels of various stiffnesses, and allowed to undergo EMT to form NCCs. Morphology, cell behaviour, gene expression and protein localisation were all analysed to determine if EMT has occurred. Observations of morphology and cell behaviour show cells on lower stiffness appearing more rounded and more epithelial than cells on a stiffer surface. The expression of EMT related genes such as Twist were shown to be upregulated while epithelial genes such as E-Cadherin were downregulated. Coupled with

immunostaining also showed an upregulation of E-Cadherin expression, this provided enough validation to view this as a plausible model for studying EMT on different stiffnesses.

Impact statement

Stem cells are one of the most important cell types and fundamental to all stages of life from the early embryo all the way through to adult lives of many organisms. One of the most important stages of life is in early development. Fundamentally this is where stem cells play the biggest role eventually differentiating into the various cell types of an organism. One population of cells known as Neural crest cells, are especially important in paving the way for many cell types. They are a highly migratory population of cells that eventually differentiate to form neurons, bone and pigment cells (Theveneau & Mayor, 2012). To do so, they must undergo a process called Epithelial to Mesenchymal Transition (EMT). Epithelial cells often adhere to neighbouring cells while mesenchymal cells display far more motility. This process is observed in not only development but also in wound healing and cancer, where is it widely studied.

Although Neural crest Cell EMT is widely studied, the exact mechanisms behind this process is not fully understood. A recent paper from the lab indicated that mechanical properties of a substrate can influence EMT (Barriga et al., 2018). This paper showed that EMT can be inhibited by softening the underlying stiffness. To begin to understand this system, we must first look at creating a robust and reproducible system. I decided to optimise the system by looking at how substrate stiffness would affect EMT in vitro through human induced pluripotent stem cells. To do so, various tasks were broken down into multiple steps. The first task was to identify a reliable protocol to recreate Neural crest cells. Secondly it was important to establish a reliable substrate protocol that had the desired stiffness in which the cells could be plated on. Finally, it was important to see how the cells would behave when placed who substrates of varying stiffness. I looked at the morphology, cell behaviour,

gene expression and protein localisation to ensure that the protocol was indeed producing Neural crest cells. Substrate protocols were tested and compared before deciding that a polyacrylamide hydrogel was the most optimal due to its accuracy and efficiency in time and cost. After plating the Neural crest cells on different substrates, the results observed were like the original Barriga paper.

This opens the possibility to now studying the exact mechanism being affected by this difference in substrate stiffness. Ideally with this knowledge it will further help our understanding of EMT and assist in other areas of the EMT field such as cancer and wound healing. At the same time, this will also further help decipher the exact mechanisms behind EMT of Neural crest cells.

Acknowledgements

I would first like to thank my supervisor Roberto Mayor for his continual support throughout the 2 years of my Masters. A huge thank you to Lucas Alvizi Cruz, who has been an amazing support at all times, without which I don't think this could have possibly been written. Also, to my family and friends who have been great throughout my degree. You've always been there to encourage and help me whenever I was down or doubting myself.

List of tables and Figures

List of Figures

Figure 1. Migration of Neural crest cells (NCCs) and their contribution to tissues, organs and structures. 20

Figure 2. An overview of EMT and MET. 23

Figure 3. Pathways regulating EMT. 24

Figure 4. Neural crest induction from iPSC. 50

Figure 5. Neural crest Cell induction analysis 54

Figure 6. Gel stiffness measurements. 56

Figure 7. Day 5 to Day 6 cell morphology differences. 59

Figure 8. Day 8 to Day 9 cell morphology differences 60

Figure 9. NBC to NCC on different stiffness 61

Figure 10. Cluster size and cell number increase over time. 64

Figure 11. 0.5 Kpa cell cluster transplant to a higher stiffness 66

Figure 12. 0.5 KPA cluster Immunofluorescence and analysis 67

Figure 13. qPCR analysis of cells. 69

List of tables:

Table 1. Table of regents and concentrations used 41

Table 2: Hydrogel recipes. All gel stiffnesses were used in all gel related experiments. 44

Table 3: Antibody list: All antibodies involved in any experiments are shown here. 45

Table 4. List of primers for rt-qPCR. All primers were obtained from Thermo Fisher. 46

List of Abbreviations

AFM= Atomic Force Microscopy

AHA= 6-Acrylamidohexanoic acid

APS= Ammonium persulfate

BMP= Bone morphogenetic protein

BSA= Bovine Serum Albumin

Dkk1= Dickkopf

ECM= Extracellular matrix

EDAC= N-Ethyl-N′-(3-dimethylaminopropyl)carbodiimide hydrochloride

EDN3= Endothelin 3

EDNRB= Endothelin type-B receptor

EMT= Epithelial to mesenchymal transition

ESC= Embryonic stem cell

FACS= Fluorescence-activated cell sorting

FGF= Fibroblast growth factors

FOV= Field of View

GF= Growth factors

HNK1= Human natural killer-1

iPSC= Induced pluripotent Stem Cell

KPA= Kilopascals

MET= Mesenchymal to Epithelial transition

MES= 2-(N-morpholino)ethanesulfonic acid

NBC= Neural Border Cell

NCC= Neural crest Cell

NHS= N-Hydroxysuccinimide

Pa= Pascals

Pax3= Paired box gene 3

SA = sympathoadrenal

SOX9,10= Sry-box gene 9,10

TEMED= Tetramethylethylenediamine

Tfap2 α= Transcription Factor AP-2 Alpha

TGFB= Transforming growth factor (TGF)-β

Wnt= Wingless-related integration site

Chapter 1: Introduction

Stem cells and early development

Stem cells are a unique population of cells that can self-renew and differentiate into other cell types. This process is fundamental to all stages of life from the early embryo all the way through to adult lives of many organisms. One of the reasons that makes stem cells so unique is the ability to have specific physiological roles that are different to that of the original cell. This could be achieved by asymmetric cell division resulting in 2 daughter cells with different fates after a single mitosis (Chhabra & Booth, 2021). At the same time, stem cells are also able to undergo symmetric cell division to form identical daughter cells, allowing for self-renewal. This ability to undergo both types of division is especially important when factoring in the early embryonic stages of development. Originally, all cells arise from a single cell known as the zygote. This cell, formed after the fusion of the egg and sperm is often totipotent, meaning that it can form all known cell types of the organism. One of the first steps of development is cleavage of the fertilized egg. Different cleavage patterns are present in different species due to the life cycles of various organisms. For example, in general, there is holoblastic (complete) and meroblastic (incomplete) cleavage types. One of the factors that have been attributed to this difference is yolk presence. Animals with little yolk such as human embryos have adopted the strategy of placental attachment leading to holoblastic cleavage. On the other hand, amphibians and birds may need to circumnavigate the presence of yolk resulting to meroblastic cleavage. After the initial rounds of cleavage, compaction then occurs in mammalian embryos which is different in the embryos of other organisms. In mammalian, Aat the 8-cell stage, many of the cells were loose and contained plenty of space within its arrangement. However, the 16 celled

ball (known as the morula in mammals) suddenly huddle together leading to the maximum contact, stabilized by tight junctions (Barlow, Owen, & Graham, 1972; Zhang & Hiiragi, 2018). It is important to note here that many differences now begin to arise between various organisms in both their developmental structure and cell behaviour. Therefore, although molecular similarities exist between the various organisms, for the purposes of this thesis, the focus will primarily be on mammalian development unless stated otherwise.

Following compaction, the embryo then forms a blastocyst (mammalian) or blastula (non-mammalian term). To do so, various layers then differentiate forming an outer shell known as the trophoblast and an inner cell mass (ICM). The trophoblast eventually forms structures that are important to providing nutrients and aid the implantation into the uterine lining (Câmara, Kastelic, & Thundathil, 2017). Importantly, the trophoblast makes no contribution to the embryo itself. The inner cell mass will eventually become the embryo and by the 64-cell stage, it has both formed a separate layer and expressed different proteins (Dyce, George, Goodall, & Fleming, 1987). After a process of cavitation, whereby the trophoblast secretes fluid into the morula, do we finally get the formation of the blastocyst. By this point 2 distinct cell layers, the epiblast (columnar epithelial cells) and hypoblast (cuboidal epithelial cells) (Niu et al., 2019) are formed.

The next morphogenetic event is called gastrulation, where the three main germ layers, ectoderm, mesoderm, and endoderm are formed. The beginning of gastrulation is through the formation of the primitive streak. For this to form the epiblast cells proliferate and migrate toward the midline of the embryo, causing both a thickening and linearisation, thus the term primitive streak (Mikawa, Poh, Kelly, Ishii, & Reese, 2004). At the cranial section of

the primitive streak, the cells elongate and form a mass of cells which form the primitive node. Epithelial cells of the epiblast then begin to migrate down and into the primitive streak via a process known as ingression. The first set of cells integrate into the hypoblast to form the endoderm. The second set of cells detach and ingress forming the mesoderm. Finally, the outer layer that remains eventually forms the ectoderm. To facilitate gastrulation, various signals must be at play.

Various signals such as *TGFB, Wnt, Nodal* and *BMP* all help to establish the primitive streak development (Faure, de Santa Barbara, Roberts, & Whitman, 2002; Skromne & Stern, 2001; Tam & Loebel, 2007). For example, *Wnt* and *TGFB* signalling together induce the formation of the primitive streak. Specifically, *Vg1* induces streak formation and then acts on *Nodal* to continue the cascade (Shah et al., 1997). Similarly, formation of the primitive streak can be regulated by *Wnt* antagonists such as *Dkk-1* (Skromne & Stern, 2001). Finally, *BMP* has also shown different levels around the primitive streak and is known to regulate its formation. Low concentrations of *BMP* are present around the streak while higher levels can be found in the surrounding embryo. In addition, it has also been shown in chick that *BMP* inhibitors can induce the formation of a streak.

Following on from gastrulation is neurulation. In this process, the embryo forms a neural tube, a precursor to the central nervous system. There are generally 2 types of neurulation, primary and secondary (Lawson, Anderson, & Schoenwolf, 2001). In primary neurulation, the underlying mesoderm instructs the ectoderm above to initially proliferate before invaginating and pinching off from the surface to form a tube. In secondary neurulation, a solid cord of cells sinks into the embryo before hollowing out to form a neural tube which is

typical of mammals. From the dorsal region of the neural tube, a specific population of cells emerges known as neural crest cells.

Neural crest cells

Neural crest cells (NCCs) have sometimes been referred to as the 4th germ layer. One of their key features is their ability to migrate and differentiate into a multitude of cell types, based on where they settle. For example, NCCs will differentiate differently at the cranial side of an embryo versus the rest. Due to these differences, NCCs are categorized into trunk, vagal and cranial populations, each serves unique purposes (Hutchins et al., 2018). Since migration is one of its defining features, it is important then to discuss the differences that exist between each population of NCCs, the genes that may govern this movement and their potency.

Trunk NCCs are usually found after the head region of the embryo and typically in the region of somites 8-28 in the chick. One of the things that makes trunk NCCs unique is their ability to migrate in 2 different ways. One manner of migration is dorsolateral which is around the periphery of the embryo, directly under the dermis. This form of migration leads to the formation of pigmented melanocytes (Erickson, Duong, & Tosney, 1992). This has been demonstrated in chick when the neural of a pigmented strain was transplanted into an albino leading to specific regions of the albino chick having coloured feathers (Rawles, 1948). The other mode of migration is the ventral pathway. This mode involves the trunk NCCs migrating ventrally through only the anterior section of the sclerotome (Figure 1a)(Bronner-Fraser, 1986). These NCCs then join with those opposite the anterior section of the somite,

forming the same structure. This can be seen in each dorsal root ganglia (one of trunk NCCs many derivatives) which is formed by 3 different NCC populations.

Some of the known genes related to this migration are *SLUG*/*SNAIL*2 and N-Cadherin. Pre-migratory NCC often express *SLUG* and inhibition of *SLUG* mRNA prevents NCC migration. N-Cadherin has also been shown to be downregulated through coordination of *BMP* signalling in migrating NCC (Taneyhill, 2008), however when the NCC begin to form aggregates, they re-express N-Cadherin.

Finally, when looking at trunk NCC, it is also important to understand their potency and their derivatives. As previously mentioned, they are known to form dorsal root ganglia, but shown to divide into adrenomedullary cells, sensory neurons and pigment cells in chick (Bronner-Fraser & Fraser, 1988).

Vagal NCCs share differences in their final differentiation, however, also share similarities in migratory pathway, having both a dorsolateral and ventral migratory path. Since vagal NCCs are known to contribute towards both the cardiac and enteric ganglia, their migration patterns share both similarities and differences with the trunk NCC. For example, they are shown to migrate dorsolateral, between the somite and the ectoderm, towards the heart (Figure 1a). At the same time, they also follow a ventral path to give rise to sensory ganglia, sympathetic ganglia and/or enteric ganglia (Kuo & Erickson, 2011). Even at later stages in chick, it has also been shown that a final wave of vagal NCCs take a dorsolateral route and gives rise to melanocytes of the skin (Reedy, Faraco, & Erickson, 1998). It is important to note here that although mouse (mammalian) migration pathways are similar to that found in chick, there are still species specific differences in timing and pathways of migration at the vagal level (Anderson, Stewart, & Young, 2006). Genetically, similarities have been

shown with other types of NCCs for example, the genes *FOXD3, Pax3, SOX10* and Transcription Factor AP-2 Alpha (*Tfap2 α*) have all been shown to impact vagal NCC numbers and lead to defects in vagal NCC-derived structures (Carney et al., 2006; Knight et al., 2003; Lang et al., 2000; Montero-Balaguer et al., 2006).

Finally with cranial (cephalic) NCCs there are again similarities and differences between the other NCC types. In general, neural crest gene regulatory network data has been compiled from several different species and has been shown to be conserved(Bronner & LeDouarin, 2012). Despite some of the previous similarities there are also differences in migration as mentioned earlier in other NCC types. For example, in chick, there are 3 major pathways taken by migratory cells. Since the trunk, vagal and sacral regions all contain somites, those were used to locate the migration pattern, however, this is not the case in the cranial section. Here, the hindbrain is instead segmented into rhombomeres along the anterior and posterior axis with different rhombomeres having different migratory patterns. Rhombomere 2 migration moves down to the first pharyngeal pouch and eventually forms the frontonasal process (Bockman & Kirby, 1984). Next, rhombomere 4 migrates towards the second pharyngeal pouch, eventually forming the vestibuloacoustic nerve and finally rhombomere 6 migrates into the 3rd and 4th rhombomere pouches to form the thymus and thyroid glands (Figure 1a) (Graham, Begbie, & McGonnell, 2004). For all this to occur, a complex molecular cascade involving genes grouped into categories such as inductive signals, neural plate border specifiers, neural crest specifiers, and neural crest effector genes are pivotal (Meulemans & Bronner-Fraser, 2004).

While these categories appear clearcut, it's essential to acknowledge their dynamic nature. Genes involved often exhibit a gradient of expression, peaking at specific timepoints rather than adhering strictly to categorical distinctions. Despite this nuance, for the sake of clarification, these genes will be grouped into these arbitrary categories. This simplification aids in comprehending the molecular choreography orchestrating NCC formation during the transformative process of neurulation.

Chronologically, after the expression of *Wnt* and *BMP*s, neural plate border specifiers, such as *PAX3* and *TFAP2A*, exhibit broad expression at the neural plate border. Notably, many of the cells expressing these specifiers serve as precursors to neural crest specifiers, exemplified by the expression of *MSX1* in *SLUG* and *SNAIL* (Tríbulo, Aybar, Nguyen, Mullins, & Mayor, 2003). NCCs subsequently express genes like *SLUG*, *SNAIL*, and *TWIST1*, collectively categorized as neural crest specifiers. In Xenopus, each neural crest specifier appears to be both necessary and/or sufficient for inducing the expression of all other specifiers. This observation highlights the presence of a comprehensive cross-regulation system (Meulemans & Bronner-Fraser, 2004).

Concluding this intricate cascade are neural crest effector genes, including *SOX9* and cadherins, pivotal for migration and multipotency. Cadherins, for instance, facilitate delamination and adhesion, while *SOX9* regulates neural crest differentiation, setting off a cascade activating cell-type-specific genes downstream (Meulemans & Bronner-Fraser, 2004). This orchestrated sequence culminates in the detachment of cells from the neural tube's summit through delamination, initiating migration to give rise to a diverse array of cell types, including neurons, bone cells, and pigment cells (Figure 1b and 1c) (Theveneau &

Mayor, 2012). Processes such as migration are often a result of Epithelial-to-Mesenchymal Transition (EMT).

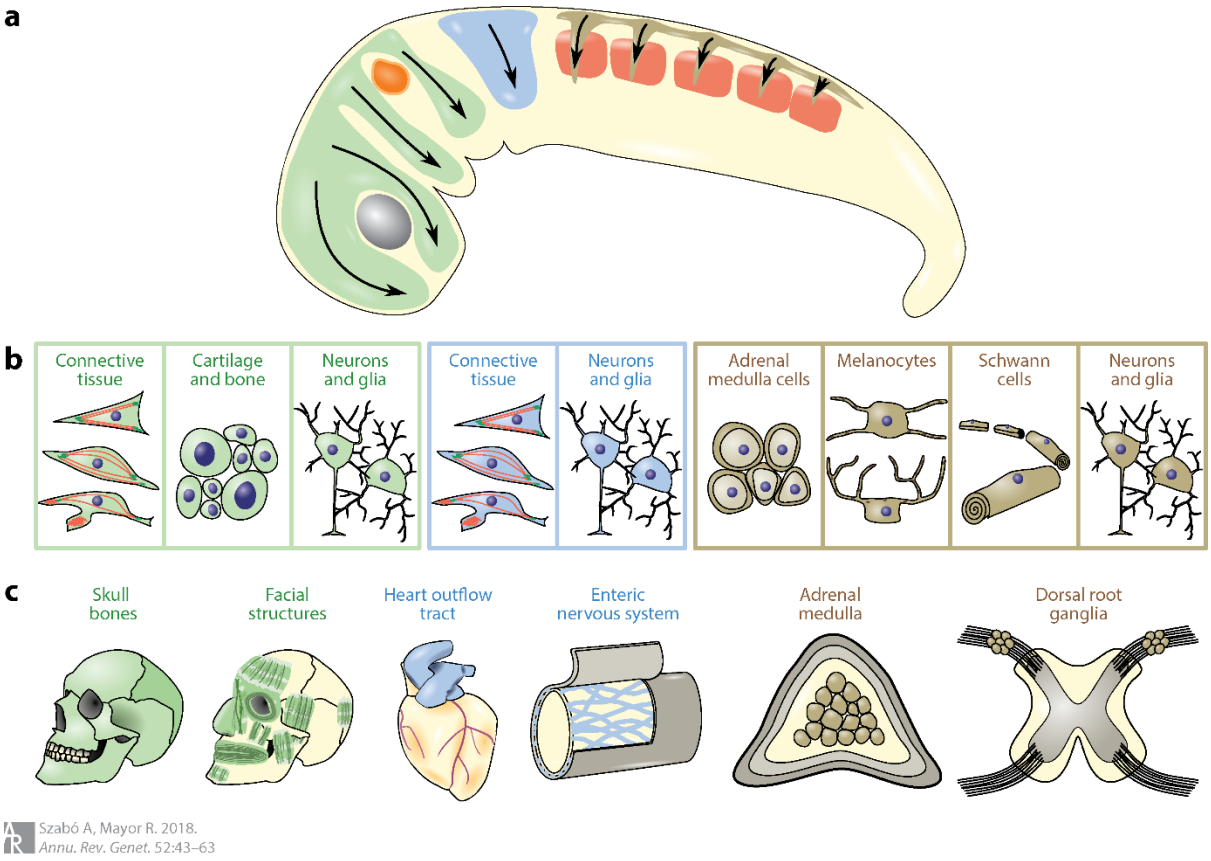

Figure 1. Migration of Neural crest cells (NCCs) and their contribution to tissues, organs and structures.
A) Migration of Neural crest cells are distinctly separated into 3 regions; Cephalic (green), vagal (blue) and trunk (red). Delamination of these regions are time and position dependent (anterior to posterior) with thicker streams more cranially and thinner streams more posteriorly. B) Cell types formed by NCCs dependent on region (trunk=brown). C) Examples of NCC organs/structures. [Adapted from Szabó et al (2018).]

Epithelial-to-Mesenchymal Transition (EMT)

To begin to understand EMT, we must first classify what it means for a cell to be epithelial and mesenchymal. The epithelial and mesenchymal states are two distinct cellular states that play critical roles in various biological processes. Epithelial cells are characterized by their ability to have a 'top' and 'bottom' (more accurately known as apical and basal polarity), stable epithelial cell-cell junctions and interactions with basement membrane (Yang et al., 2020). These features are crucial for maintaining the integrity and function of epithelial tissues. Adherens junctions, which utilize E-cadherin as a calcium-dependent cell-cell adhesion molecule, play a pivotal role in cell-cell interactions by anchoring the actin cortex to the apical side of the cell (Figure 2) (Takeichi, 1977). This allows for the transmission of contractile forces through the actomyosin complex between adjacent cells (Martin & Goldstein, 2014). Tight junctions, composed of proteins from the claudin family, act as a diffusion barrier, preserving the polarity of the cell (Förster, 2008). Collectively, these various features ensure the maintenance of the epithelial state of a cell.

In contrast, mesenchymal cells are far more migratory and express a variety of different surface proteins versus those in the epithelial state. E-cadherin for example is shown to be expressed in epithelial cells and repressed in mesenchymal cells (Vestweber & Kemler, 1985). Transcription factors such as the *SNAIL* family are predominantly found in mesenchymal cells and turned off in epithelial cells (Wang, Shi, Chai, Ying, & Zhou, 2013) .

Epithelial and mesenchymal cells can alternate between the two forms via a process called Epithelial to Mesenchymal Transition (EMT). The inverse of this process is Mesenchymal to Epithelial Transition (MET). Both processes play a central role in numerous biological

processes most notably, wound healing, cancer, and embryonic development (Barriere, Fici, Gallerani, Fabbri, & Rigaud, 2015). However, it has been discovered that there may be a potential third state called partial EMT. This is where epithelial markers are not completely lost, and mesenchymal markers are not completely gained. In wound healing, EMT occurs in the epithelial cells near the wound site, allowing them to fill the gap created by the injury. For re-epithelialisation of mammalian skin for example, proliferation, differentiation, and collective migration of keratinocytes must occur. Directly around the wound, the cells change shape from polarized cuboidal to flattened and elongated (Odland & Ross, 1968). Reduction of adherens junction components such as E-cadherin lead to the appearance of intercellular gaps (Coulombe, 1997; Haensel & Dai, 2018). Previously mentioned genes such as Wnt have also been shown in hair follicle regeneration for large wounds (Ito et al., 2007). There is also evidence of the *SNAIL* family particularly *SLUG* (*SNAIL*2) being involved in vivo for cutaneous wound healing. Its expression is shown to be elevated in keratinocytes at the edges of wounds in vivo and in vitro. *SLUG* deficient mice were shown to lack epidermal migration within 72 hours after wounding. Cells at the leading edge were shown to lack prominent protrusions (Arnoux, Côme, Kusewitt, Hudson, & Savagner, 2005; Hudson et al., 2009). Wound healing usually concludes with the 2 migrating fronts of keratinocytes contact one another. This halts migration and regeneration (Haensel & Dai, 2018).

However, partial EMT has also been put forward as a part of wound healing (Arnoux et al., 2005). One argument is that although there is a loss of epithelial traits, which is key to keratinocyte activation, very few mesenchymal features are gained (Yan et al., 2010). Similarly, EMT genes are not present as part of the leading edge in the migratory cells (Aragona et al., 2017).

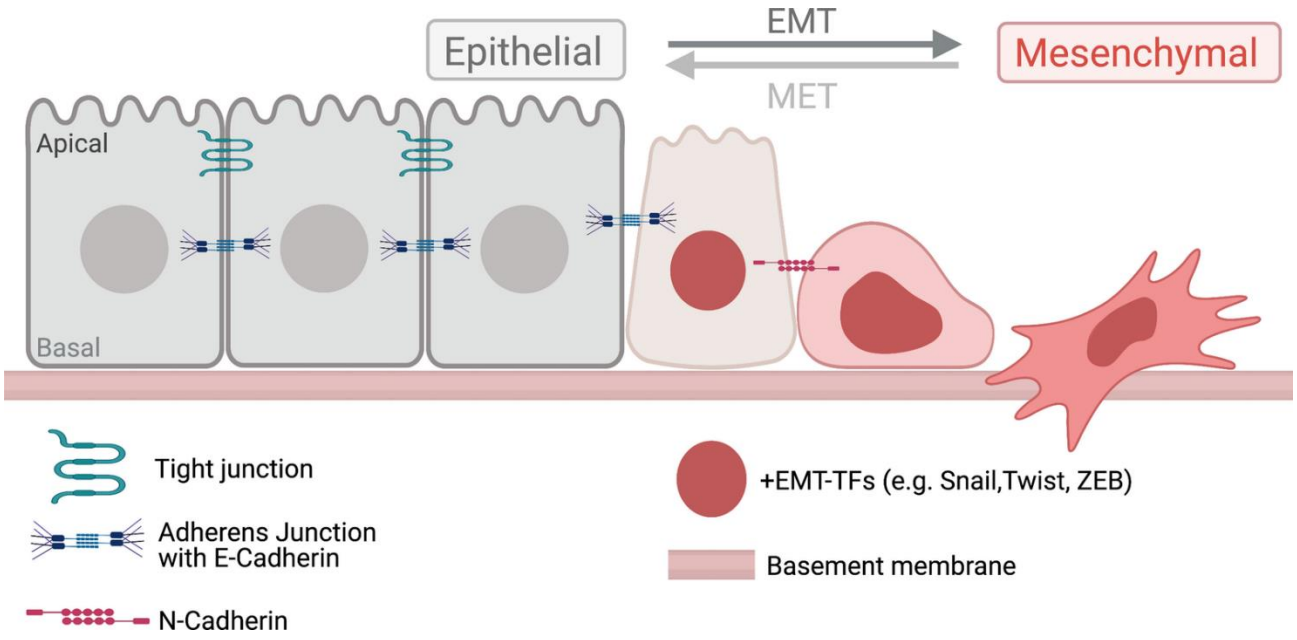

Figure 2. An overview of EMT and MET.

Epithelial to mesenchymal transition (EMT) is a process in which epithelial cells lose their characteristics, such as apical-basal polarity, tight junctions, adherens junctions, downregulating E-Cadherin and become more mesenchymal. As cells become more mesenchymal, they upregulate N-Cadherin as well as EMT transcription factors such as *SNAIL* and Twist. Mesenchymal to epithelial transition (MET) is the opposite effect. [Adapted from A. Mack (2021.)]

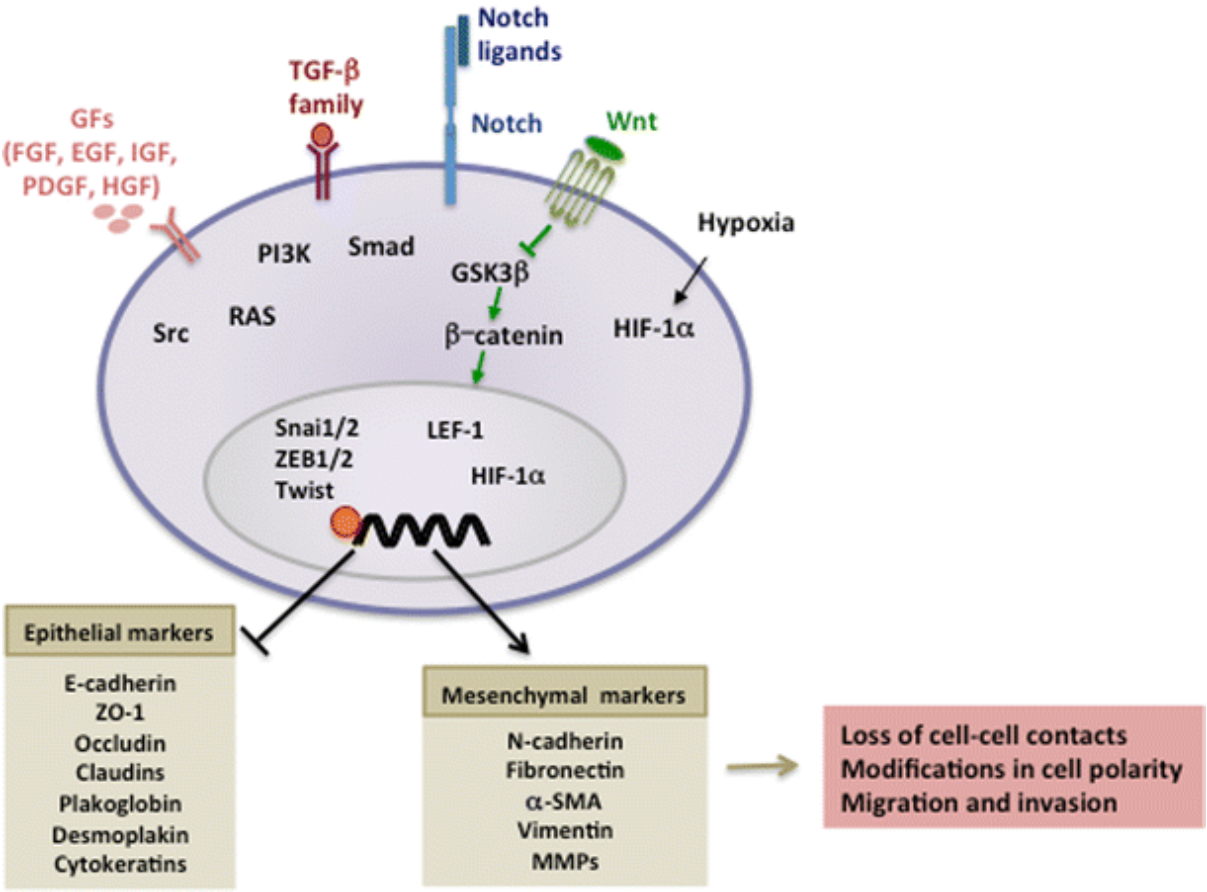

Figure 3. Pathways regulating EMT.

Extracellular factors such as growth factors (GF) and other molecules interact with various intracellular molecules such as β-Catenin. This leads to activation EMT transcription factors such as Twist and Snail. Eventually, this inhibits epithelial markers such as E-Cadherin and activates mesenchymal markers such as N-Cadherin. [Adapted from Germani et al., 2015]

In cancer, EMT is associated with the metastasis of tumour cells to other parts of the body. Discovered early in the 80s (Ribatti, Tamma, & Annese, 2020; Schor & Schor, 1987), benign tumours can acquire metastasizing and infiltration properties. This usually occurs with most tumours that begin to move away from their benign states, similar to many previously mentioned processes, the cells lose their cell-cell adhesion and cell polarity with transforming growth factor beta (TGF-β)/Smads pathway being potentially the strongest EMT inducer (Xu, Lamouille, & Derynck, 2009). *SNAIL*1 has also been shown in human carcinomas such as colon cancer as an inducer and Twist involved in maintaining the mesenchymal phenotype (Figure 3). It is also correlated with malignancy of induced breast tumours and tumour relapse (Moody et al., 2005).

However, especially in cancer, not all EMT is complete (Kisoda et al., 2022). Cancers cells that have undergone partial EMT become a lot more 'aggressive', leading to invasion, metastasis and drug resistance (Pastushenko et al., 2018). To achieve this, cancer cells must be expressing both epithelial and mesenchymal markers concurrently. (Shibue & Weinberg, 2017). Typically, cancer stem cells that that survive in blood exhibit both types of markers and exit the bloodstream more efficiently. (Yu et al., 2013). Additionally, effective metastasis is usually when cancer cells neither completely lose their epithelial state not completely gain mesenchymal properties. In fact, by retaining partial EMT, they can more effectively undergo collective cell migration by retaining epithelial properties. Mesenchymal properties will aid with attachment to the Extracellular matrix (ECM). Therefore, cancer cells with partial EMT are believed to be of higher metastatic risk (Saitoh, 2018).

Finally, Epithelial-to-Mesenchymal Transition (EMT) emerges as a pivotal phenomenon in early development as previously mentioned, contributing to the formation of both the

mesoderm and neural crest cells. However, it is important to note that it is not known if partial EMT does exist in early development since most known EMT has been shown to be complete (Saitoh, 2018).

In terms of complete EMT, one of the first examples occurs during gastrulation when epiblast cells facilitate their migration between the epiblast and hypoblast layers and ultimately form the mesoderm (Y. Nakaya & G. Sheng, 2008). Depending on the organism, different animals undergo gastrulation differently. For example, in sea urchin this occurs in 2 phases. Primary mesenchymal cells give rise to the larval skeleton and ingress from the vegetal plate in the blastula stage embryo prior to formation of the archenteron (Yukiko Nakaya & Guojun Sheng, 2008). Before undergoing ingression the vegetal plate cells are epithelial with septate and adherens junctions, basement membrane and apico-basal polarity (Balinsky, 1959; Savagner, 2007). However, for Drosophila, no basement membrane exists, however they retain all other epithelial properties (Oda, Tsukita, & Takeichi, 1998). These cells then invaginate more as a topological rearrangement of an intact epithelium. This then results in the mesoderm cells adopting a more mesenchymal morphology before undergoing EMT (Leptin & Affolter, 2004). However, for animals like zebrafish, no EMT generally occurs. This is seen in the involution movement at the blastoderm margin where the enveloping layer flattens due to radial cell intercalation (Warga & Kimmel, 1990). No epithelial structure is visible currently. Instead, cadherins mediate the differential cell adhesion and tensile force differences between the germ layers end up contributing to germ layer segregation (Kane, McFarland, & Warga, 2005; M. Krieg et al., 2008).

EMT is also observed during the formation of the neural tube. Initially the edges of the neural plate grow to form the neural groove. The neural crest s located on either side of the neural groove then grow and eventually connect to form the neural tube. During this process, the NCCs undergo EMT and disperse in the mesoderm, playing an important role in the development of various tissues and organs covered earlier. (Figure 1A-D) (Rogers, Saxena, & Bronner, 2013).

Thus far, the primary emphasis has centred on understanding protein-protein interactions and gene regulatory networks in the context of EMT. Nonetheless, recent investigations reveal that additional factors play integral roles in interacting with EMT dynamics. Notably, it has been demonstrated that, as developmental processes unfold, the stiffness of the mesoderm beneath the NCCs undergoes a progressive increase. Intriguingly, when the stiffness of the mesoderm was deliberately reduced, it resulted in a consequential decrease in NCC migration (Barriga et al., 2018). Overall, this introduces the notion that mechanical cues exert a tangible impact on the intricacies of EMT during early development.

Mechanobiology

Mechanobiology is the study of how physical factors regulate a wide range of biological activities, including morphogenesis, cell migration, polarization, proliferation, and single molecule behaviour (Lim, Bershadsky, & Sheetz, 2010). Broadly speaking this can range from the muscle mass gained lifting weights to muscle mass lost when astronauts return from space. Sound waves are converted into vibrations in the ears, utilising mechanobiology. The term is often confused with ‘biomechanics’ which is the mechanical aspect of tissues or

biological systems while mechanobiology deals with the cascade of biological events mediated by mechanical forces (Kim, 2021).

To understand mechanobiology, we must first understand the term stiffness of a material and whether it is soft or hard. Various tissues and organs also all have varying stiffnesses. For example, while most liquids sit below 50 Pascals (Pa) (Butcher, Alliston, & Weaver, 2009), tissues such as fat and lung tissue sit around 200 Pa (Cox & Erler, 2011). On the other hand, organs such as the brain sit between 1Kpa~4Kpa and the heart sit at around 10-15Kpa (Handorf, Zhou, Halanski, & Li, 2015). On the more extreme end, cartilage and bone move into the range of over 1 gigapascal. Bone requires this stiffness to provide structure and protect internal organs while the heart must be both elastic enough, but also hold its structure to maintain its function. For the purposes of this thesis, 'soft' will generally refer to stiffnesses <1 KPA while anything higher would be termed 'hard'.

At the molecular level, one of the key aspects of mechanobiology is the conformational changes and protein interactions that play a pivotal role, influencing gene transcription. This usually involves a myriad of mechanosensing and mechanotransduction implicating integrins, ECM and the cytoskeleton. Integrins for example recruit more than 150 proteins to the cell ECM network (Jansen et al., 2015). These molecular events cascade into the formation of protein complexes and modules that orchestrate critical cellular functions, including migration, force transmission through cell adhesions, and the transportation of materials, including ions, both within and between cells (Kim, 2021).

Various techniques have also emerged to aid detection of these mechanical forces. This ranges from measurement tools to the manufacturing at the nano/micro level. The invention of the atomic force microscope (AFM) in 1980 (Binnig, Quate, & Gerber, 1986) emerged as one of the major tools in science and engineering but also mechanobiology. The AFM allowed for force to be applied and measured, providing information on both morphological and mechanical characterization of biological systems (Michael Krieg et al., 2019). With the more recent invention of super-resolution microscopy and single molecule imaging techniques, it is now possible to study mechanobiology at a more molecular level, particularly looking at proteins and various molecular interactions controlled by mechanical forces (Shamsan & Odde, 2019).

One of many uses of mechanobiology is the potential application in drug development and translational medicine. It is now known that alterations in cellular mechanics can either stem from or contribute to various diseases, spanning cancer, infectious diseases, cardiovascular ailments, and the aging process (Suresh et al., 2005). A portfolio performance of AstraZeneca from 2005 to 2010 has shown that despite sufficient concentration, duration and drug exposure, drugs behaved differently to *in situ* compared to the assay systems (Cook et al., 2014). One such explanation is the oversimplified mechanical microenvironment of cell culture that was used to test the drugs. One potential avenue to fixing this issue are some recent advances by Ingber and colleagues using 'organ-on-a-chip' whereby cell cultures are subjected to cyclical strain such as breathing, peristalsis, etc, giving a more applicable use of human cell cultures for trialling drug discovery (Jang et al., 2013). Crucially, it is paramount to know what exactly the forces that are generated and their effect on a system.

Some of the forces acting on cells include stress, strain and the aforementioned, stiffness. For example, smooth muscle is subject to both stress and strain. Extrinsic forces may lead to changes in its stiffness, at the same time, intrinsic forces of the muscle may be used to control organ function (Krishnan, Park, Seow, Lee, & Stewart, 2016). This is easily observed in asthma patients. Patients will often struggle to relax smooth muscle in response to mechanical perturbation (Skloot, Permutt, & Togias, 1995). This can lead to force and stiffness in airway smooth muscle (Raqeeb, Jiao, Syyong, Paré, & Seow, 2012). However, this smooth muscle stiffness can also be used as a target for anti-asthma drugs. Fibroblast growth factor 2 (FGF2) has been shown to reduce the stiffness of transforming growth factor (TGF)-β in cultured airway smooth muscle cells (Schuliga et al., 2013). This is just one of many molecular factors that can impact a cell.

When looking at the molecular level, various targets have been proposed. Some of this research has focused on single molecules engaged in motor-track interactions and investigations into mechanosensitive ion channels. The motor track ion system, a composite of actin and microtubule-based systems, has been classically illustrated through the dynamic interplay of myosin "walking" along an actin track, facilitating muscle contraction, and the kinesin protein similarly navigating along a microtubule system (Mikhailenko, Oguchi, & Ishiwata, 2010). Additionally, mechanosensitive ion channels, which are integral membrane proteins forming pores, exhibit responsiveness to mechanical stimuli applied to the cell membrane. By transitioning between closed and open conformations, these channels facilitate the passage of ions and other solutes across cellular membranes. An exemplar in this category is Piezo1, where, upon mechanical stimulation, calcium ions flow into the cell, initiating a biochemical cascade that interlinks mechanical forces with

biochemical signalling (Canales Coutiño & Mayor, 2021b). Notably, Piezo1 has been demonstrated to regulate *Rac1* and focal adhesion dynamics *in vitro*, crucial activities essential for counterbalancing inhibitory signals, such as *Sema3A* and *Sema3F*, during neural crest migration *in vivo* (Canales Coutiño & Mayor, 2021a).

Furthermore, mechanosensitive ion channels such as *YAP/Taz* have shown to impact potency (their ability to form multiple differentiated lineages) and self-renewal, affecting both embryonic and adult stem cells alike (Heng et al., 2020). An example of this is the downregulation of *YAP* in mouse embryonic stem cell (ESC) differentiation with YAP silencing leading to loss of ESC pluripotency (Lian et al., 2010).

Recently the effect of altering the underlying stiffness of NCCs has been shown (Barriga et al., 2018). In this paper they were able to demonstrate the importance of high stiffness leading to NCC EMT and overall migration. Notably, ablations and myosin light chain inhibitions lead to a softening of the underlying mesoderm, hence inhibiting NCC EMT. Conversely, an early increase in tissue stiffness leads to premature NCC migration. Despite these insights, the paper provides limited details on the underlying mechanism governing these changes in cell behaviour. The responsible genes remain largely unexplored. To delve into this aspect, it is important to establish the role that stiffness plays in EMT. Most research has shown a connection between matrix stiffness and EMT for example in pancreatic cancer cells (Rice et al., 2017). Rice et al. discovered that increasing stiffness (to values of 1, 4 and 25 Kpa,) not only increased the rate of EMT, but also chemoresistance to various drugs. Overall, although an effect is known, little is known about the exact pathway in which this system is regulated.

It is important to look at why NCC research may be able to provide insight into the mechanics impacting EMT.

Significance of NCC

One of the things that has not been discussed is the potential for what can go wrong with NCC migration. As shown in Figure 1, NCCs can be found spanning the entire length of the organism. Therefore, diseases will display differently depending on which NCC population is affected. For example, when looking at the trunk NCC, sympathoadrenal (SA) cells are known to differentiate into both sympathetic neurons and neuroendocrine cells. These cells are especially important for the adrenal medulla, where defects can lead to pheochromocytoma or neuroblastoma (Fung, Viveros, & O'Connor, 2008). Similarly, defects in Vagal NCCs are associated with severe developmental issues, such as Hirschsprung's disease (Puri & Shinkai, 2004). Genetically this involves mutations in NCC related genes, leading to the absence of Ret receptor tyrosine kinase. This leads to a lack of enteric neurons forming which results in Hirschsprung's disease. Similarly Waardenburg syndrome can also form from a disrupted enteric NCC migration (Butler Tjaden & Trainor, 2013). This can occur when pathways such as the EDN3-EDNRB are disrupted (Butler Tjaden & Trainor, 2013). Finally, since cranial NCCs, for instance, contribute to the ‘face’ and the development of cranial neurons, connective tissues, and facial bones (Gilbert, 2000). Many known defects such as the formation of cleft palate due to a loss of E-cadherin (Alvizi et al., 2023), but also Treacher Collins syndrome (Treacher-Collins, 1900). This is often characterized by incomplete development of the facial bones leading to more widely spaced teeth that are mispositioned or even reduced. They have also been shown to have irregular or absent

auditory with fusion of the ear bones resulting in hearing loss (Phelps, Poswillo, & Lloyd, 1981).

Moreover, other than further understanding diseases in early development insights gained from NCC research can also prove to be valuable in cancer research where certain genes implicated in metastasis share roles with neural crest cells (Gallik et al., 2017; Kulesa, Morrison, & Bailey, 2013). From as early as Wnt and BMP, both are extensively studied in both cancer and early development. In addition to BMP for example, NC induction requires both FGF (Fibroblast growth factor) and Wnt (García-Castro, Marcelle, & Bronner-Fraser, 2002; Mayor, Guerrero, & Martínez, 1997). However, at the same time Wnt is widely studied in relation to cancer due to its interactions with the MYC family. For example, when the canonical Wnt pathway is cancer cells, genes of the MYC family are transcribed (Rennoll & Yochum, 2015). In light of the notion that Wnt signalling-mediated effects may transpire through interactions with N-MYC (Duffy et al., 2016), this leads to the idea that overactivation of canonical Wnt signalling supports self-renewal of cancer cells (Tammela et al., 2017). Looking forward in developmental time, canonical Wnt signalling also promotes the delamination of NCCs. This cascade then leads to activation of signalling activities for genes such as SLUG/SNAIL, FOXD3 and the SoxE family, SOX9 and SOX10 (Cheung & Briscoe, 2003; Cheung et al., 2005). With cancer cells, this is often through metastasis where they will undergo a similar delamination. Similarly, cancer cells will activate SLUG/SNAIL which are responsible for repressing cell-cell adhesion molecules such as E-Cadherin (D. Zhang et al., 2014).

Looking into genes in the SNAIL family, we see further interactions that relate to both cancer and early development. Although SNAIL is not generally required in mice (Murray & Gridley, 2006), knockdown of SNAIL2 inhibits NCC migration in Xenopus (Carl, Dufton, Hanken, & Klymkowsky, 1999) and plays important roles in neural crest development (Aybar, Glavic, & Mayor, 2002). Similarly, its overexpression is important to induce NCC specification in chick (Sauka-Spengler & Bronner-Fraser, 2008). However, SNAIL is also known to play multiple roles in cancer as well. For example, SNAIL has shown to promote cancer cell proliferation via BIRC3 (Rho, Byun, Kim, & Lee, 2022) as well as maintaining neuroblastomas in an invasive state of malignancy and favours dissemination (Delloye-Bourgeois & Castellani, 2019). This shows not only the relevance of studying NCCs but also the potential applications of such knowledge in both early development and later stages, notably in cancer.

Here is it important to note that as with NCCs, Epithelial-to-Mesenchymal Transition (EMT) is not a simple process and has been shown in both in vitro and in vivo models. Some cancer cells have been shown to downregulate cadherins yet do not appear to be migratory (Bronsert et al., 2014). Similarly, some breast cancer populations have shown to contain both epithelial and mesenchymal states or incomplete EMT (Grosse-Wilde et al., 2015).

Creating a system to study the role of stiffness on EMT

With the recent paper published by Barriga et al. 2018, it can be concluded that EMT can be controlled by mechanics although the precise underlying mechanisms remains elusive. To study the role of stiffness on EMT the establishment of a robust experimental system

becomes imperative. This necessitates a careful consideration of the two primary avenues for studying neural crest dynamics: *in vivo* and *in vitro*.

As with the Barriga paper, the studies were conducted *in vivo* on *Xenopus Laevis*. Opting for this approach provides notable advantages, particularly the ability to closely examine the intricate interactions between the stiffening mesoderm and Neural crest cells (NCCs). This choice also facilitates a nuanced understanding of the developmental timing associated with these crucial events. However, often with *in vivo* research there are also disadvantages. For example, there's a challenge in exercising precise control over the *in vivo* environment, exemplified by the variability observed in mesoderm stiffness measurements over time (Barriga et al., Figure 1h). Another concern is the overall ethics of using animals in research despite many of the strict regulations and guidelines for their treatment. Hence, it may be better to instead look at an *in vitro* model. The key lies in establishing a reproducible and reliable *in vitro* model, serving as a foundational platform for subsequent investigations into potential mechanisms.

Conversely, the *in vitro* approach offers distinct advantages in terms of optimization. The ability to meticulously control culture conditions minimizes variability, circumventing potential confounding factors arising from differences between Xenopus embryos. Moreover, ethical considerations are substantially diminished, particularly when employing induced pluripotent stem cells (iPSC) derived from human adult cells. Although the *in vitro* environment may be criticized for its oversimplified nature and limited tissue interactions, these aspects are inconsequential for the current thesis focus. Given the primary objective of constructing a platform for the eventual study of NCC behaviour on substrates of varying

stiffness, a simplified environment proves instrumental. Furthermore, the elimination of extensive tissue interactions mitigates potential noise in the experimental setup, facilitating clearer interpretation of results. After careful consideration of both *in vivo* and *in vitro* methodologies, it made the most sense to adopt the use of *in vitro* cell culture.

The next question is the cell line to use. To understand what protocol to choose for this project, it is important to navigate through the history of in vitro differentiation of NCCs. One of the first few methods for maintaining and differentiating cells were through maintenance of ESCs via feeder layers (Richards, Fong, Chan, Wong, & Bongso, 2002). These feeder layers allowed for the ESCs to continuously proliferate and maintain their pluripotency (Llames, García-Pérez, Meana, Larcher, & del Río, 2015) allowing for more consistent study of this cell type. As this method became more well established, steps were then further taken for differentiating these cells into various cell lineages. One of these lineages are NCCs, with the earliest example by Chambers et al. demonstrating a protocol that allowed for differentiation towards neural progenitor, including NCCs. However, this protocol still relied on a feeder layer and often quite complicated. As more research was conducted on differentiating pluripotent cells, factors that were secreted by these feeder cells were eventually discovered, leading to feeder free protocols being used (Zeltner, Lafaille, Fattahi, & Studer, 2014). Nevertheless, many of these protocols still faced issues with FACS sorting being required to separate the NCC from other cell types. As more refinement occurred, these protocols also increased in speed, with some protocols only requiring 5 days to fully differentiate into NCCs (Leung et al., 2016) while more traditional protocols would require more than 20 (Chambers et al., 2009). Although this did show a much higher rate of efficiency, throughput was still an issue with Leung et al. reporting

‘63.1±9.6% SOX10 positive, 78.6±7.9% PAX7 positive and 84.4±7.6% TFAP2A positive cells’ in their immunostaining. This leads to potential variation in the cells and errors that could occur further down the line if this protocol was used. Similarly, for our purposes, this protocol also lacked a distinct NBC phase due to the speed of derivation. Therefore, a slower protocol with a high throughput was required. One such protocol by Kobayashi et al., demonstrated both these properties. It was reported that flow cytometry showed 93.94% of cells being double positive for NCC markers p75 and HNK1. Further analysis of immunofluorescence also showed 97.46% of FOXD3+ and 99.41% SOX10+ cells (Kobayashi et al., 2020). This higher throughput and slower differential rate (more closely mimicking that of a human embryo) made it a more suitable method for the purposes of this thesis.

Finally, it is noteworthy that a large variety of protocols exist for a variety of different stiffnesses. This ranges from more commercially bought ready-made silicon based gels all the way to more complicated stiffness altering gels based on light (Özkale et al., 2022). All of these can serve as potential options. However, once various factors such as accessibility and regulation are considered, then it would be far more logical for the gels to be made within the lab. To do so, a few more factors must now be determined. For example, due to the nature of iPSC, coating a substrate surface is necessary for the iPSC to attach. In that scenario, a few different protocols are viable. One of those protocols utilises Sulfo-SANPAH as a crosslinker for polyacrylamide gels (Pelham & Wang, 1997). This allows for ECM proteins such as fibronectin to bind, however, the gels are prone to being unstable and can result in inconsistent effect of gel stiffness towards cellular responses (Kandow, Georges, Janmey, & Beningo, 2007). Alternatively another method for crosslinking is with AHA (6-Acrylamidohexanoic acid) (Beningo & Wang, 2002) which is far less toxic and much easier to

prepare, forgoing the use of UV light. This method is like Sulfo-SANPAH whereby it creates various anchorage to bind the ECM proteins (Labouesse et al., 2021). Due to the various benefits this method held, it became the preferred method.

Aims

The main purpose of this project is to establish a suitable system to study the role of stiffness on EMT. To achieve this, the following steps must be taken:

1. Identify a suitable cell protocol for *in vitro* experiments.
2. Optimize a gel protocol to place the cells on
3. Plate the cells on the gels to monitor cell behaviour.

Chapter 2: Materials and methods

Name of Reagent	**Company obtained**	**Concentration/amount (if applicable)**
Fibronectin	Sigma Aldrich (MERCK)	50 µg/ml
E8 Media	Thermo Fisher	-
E6 Media	Thermo Fisher	-
Normocin	Invivogen	50 mg/µL
Dulbecco's Modified Eagle Medium (DMEM)	Thermo Fisher	-
Rock Inhibitor (Y-27632)	Stem Cell Technologies	5 µM
Fibroblast Growth Factor-Basic human (bFGF)	Sigma Aldrich (MERCK)	8 ng/mL
SB-431542	Stem Cell Technologies	20 µM
CHIR99021	Stem Cell Technologies	1 µM
Ethanolamide	Fisher Scientific	50 mM
6-Acrylamidohexanoic acid (AHA)	TCI chemicals	48mM
N-Ethyl-N′-(3-dimethylaminopropyl)carbodiimide hydrochloride (EDAC)	Sigma Aldrich (MERCK)	0.2M
N-Hydroxysuccinimide (NHS)	Thermo Fisher	0.5M
2-(N-morpholino)ethanesulfonic acid (MES) buffer	Sigma Aldrich (MERCK)	-
Acetic Acid	Fisher Scientific	1:16
Bind Saline	GE Healthcare	1:16
Ethanol	Honeywell	14:16
Acrylamide 40% (µl)	Bio-Rad	See Table 2 for concentration
Bis-Acrylamide 2% (µl)	Bio-Rad	See Table 2 for concentration
Tetramethylethylenediamine (TEMED)	Thermo Fisher	1:100
Ammonium persulfate (APS)	Thermo Fisher	1:200
PBS 1x	Fisher Scientific (Oxoid)	-

Paraformaldehyde	Sigma Aldrich (MERCK)	-
CryoStor CS10 Cell Freezing Medium	Stem Cell technologies	-
Matrigel	Corning	50 µg/ml
Bovine Serum Albumin (BSA)	Sigma Aldrich (MERCK)	Dependent on Immunostaining protocol
Accutase	Stem Cell technologies	-
Triton/Tween	Thermo Fisher	1:1000
VECTASHIELD	Vectorlabs	-
Superscript Vilo Mastermix	Thermo Fisher	-
PowerUP SYBR Green PCR Master Mix	Thermo Fisher	-
Primers	Thermo Fisher	200nM

Table 1. Table of regents and concentrations used

Fibronectin/Matrigel coated plates

Fibronectin/matrigel is diluted to 50 µg/ml in PBS from a stock concentration of 1mg/ml. Wells/Dishes/gels are incubated with Fibronectin at 37 °C, 5% CO2 for at least 10 min. After incubation, the fibronectin is removed and media from the appropriate cell type is added to the dish.

hiPSC and NBC thawing and maintenance

hiPSC are thawed via prewarming with E8 medium supplemented with Normocin (referred to as hiPSC media henceforth). The tubes were centrifuged and hiPSC collected followed by removal of supernatant without disturbing the cell pellet. Cells were then resuspended in hiPSC media.

Cell Passaging

Supernatant is removed and washed gently with 1xPBS (2ml in a 60mm culture dish). The supernatant is again removed and the cells are disassociated with StemPro Accutase (1ml in a 60mm culture dish) and incubated at 37 °C and 5% CO2 for 2–5 min. The Accutase is then diluted with Dulbecco's Modified Eagle Medium (DMEM) at the same volume as the Accutase (1ml in a 60mm culture dish for example). The culture dish surface was gently rinsed before transferring the suspension to 15ml conical tubes to centrifuge for 5min at 300 RPM. The supernatant was then removed without perturbing the cell pellet. The pellet was then resuspended in the appropriate media before being plated on the appropriate surface. All media is supplemented with 5 µM concentration of RocK inhibitor. The dishes were then incubated at 37 °C and 5% CO2. After 24 hours, the supernatant is removed and media appropriate to the cells are then added.

Cell cryopreservation

The procedure for cryopreservation is the same protocol as what is mentioned in 'Cell Passaging' with the exception that once the cell pellet is created, the cells are then resuspended in CryoStor CS10 Cell Freezing Medium at 500 µL/1.5 mL cryovial. They are then stored in a −80 °C freezer for at least 4 h before further use.

Differentiation of human induced pluripotent stem cells (iPSC) to NBC

To begin the differentiation process, hiPSCs are plated onto Matrigel-coated 35mm Corning culture dishes. The seeding density was approximately $2.5*10^5$ at around $2.8*10^4$ cells/cm^2 and hiPSC media is added. On the first day of plating, ROCK Inhibitor (Y-27632) is added to the E8 media. On the following day, E6 media is supplemented with Normocin (referenced henceforth as NBC media) which marks Day 0 of the differentiation process. For the next

four days, the total media is changed daily. By day 4, cells should display an NBC identity and can be collected for NCC differentiation. The main purpose of this protocol is to establish an epithelial layer of cells to then study EMT. *(Adapted from Nani et al.)*

Human Cell lines used:

Initially the cell line used was the cell line F8799-1c1 as detailed in Kobayashi et al. However, due to high passage number, this was switched to the USCBi001-A at the following link:

https://hpscreg.eu/cell-line/USCBi001-A

All experimental results between the 2 cells lines were initially compared and no significant differences were observed morphologically or by qPCR analysis.

Differentiation of NBC to NCC

To initiate the NCC induction process, cells are harvested from the iPSC-NBC protocol as shown above (either fresh or frozen) and cultured on Matrigel-coated culture dishes. On the first day of plating, NBC media is supplemented with ROCK inhibitor (Y-27632). The next day, the total media was switched to NCC media (which consists of E6 media, bFGF (a *BMP* inhibitor), SB431542 (a *BMP* inhibitor), CHIR99021 (a GSK3 inhibitor and Wnt activator) and Normocin. It will now be referenced as NCC media). This marks Day 0 of the NCC induction process. The NCC media was changed daily for the next 15 days, and then split every 2-3 days onto new Matrigel-coated wells/dishes. For cells to be cultured on polyacrylamide gels, the cells were split onto freshly made gels and incubated for 10 minutes with NCC media. This protocol allows us to establish a population of cells that have undergone EMT and are fully mesenchymal. *(Adapted from Nani et al.)*

Gel protocol

To prepare coverslips for use, they are soaked in a Bind-Saline solution (made up of acetic acid, bind saline, and ethanol) for a minimum of three hours. After soaking, the coverslips were washed with ethanol and ensured that both sides are completely dry. Using the table provided below, appropriate ingredients were added into a 0.5 ml tube, making sure that TEMED and APS are added last. Next, an appropriate amount of the gel solution was plated onto a flat surface and then the coverslip was placed on top of the gel solution. This was left to polymerize for 30 minutes before the coverslip was carefully removed and briefly washed it in methanol. After washing, the coverslip was transferred to 1xPBS and allowed to soak. Next, the AHA was activated by placing the hydrogels in an EDAC-NHS-MES buffer for 30 minutes before being washed again in 1xPBS. The hydrogels were coated with 50 µg/ml Fibronectin overnight, then blocked with an ethanol amine solution and washed with 1xPBS. These gels were stored at 4° for a maximum of 1 week before use. Finally, the gels were incubated in the appropriate cell media for 10 minutes before use at 37°C. (Adapted from Labousse et al.)

E (kPa)	**Acrylamide 40% (µl)**	**Bis-Acrylamide 2% (µl)**	**AHA 2M (µl)**	**H_2O (µl)**	**TEMED (µl)**	**APS(µl)**
0.5	37.5	15	12	447.5	2.5	5
0.75	35	30	12	415.5	2.5	5
160	200	150	12	130.5	2.5	5

Table 2: Hydrogel recipes. All gel stiffnesses were used in all gel related experiments.

Immunostaining:

Excess media was aspirated before the cells were briefly washed in PBS 1x and then washed in PBS 1x + 0.1% Triton. Next, the cells were fixed with 4% formaldehyde in PBS for 15 minutes. After fixing, the cells were blocked with a solution of 5% BSA in PBS with 0.1%

Tween (PBT) for one hour. The coverslips were washed with PBT before being incubated with primary antibodies (Table 2) in the blocking solution for one hour at room temperature. Following the primary antibody incubation, the coverslips were washed twice with PBT and then incubated in secondary antibodies (Table 2) for one to two hours again at room temperature. After incubation with the secondary antibodies, the secondaries were removed and then incubated with DAPI for 15 minutes before being washed twice with PBT. Finally, the coverslips were mounted onto microscope slides using VECTASHIELD mounting media.

Primary antibodies:	**Concentration used**	**Secondary antibodies:**	**Concentration used**
E-cadherin (mouse) [DSHB]	1:60	Donkey anti mouse 488 (Abcam)	1:200
HNK1 (rat) [DSHB]	1:60	Donkey anti rat 647 (Abcam)	1:200
		DAPI	1:1000

Table 3: Antibody list: All antibodies involved in any experiments are shown here. All sources are underlined

Real-time quantitative PCR

1 µg of RNA was extracted using the Monarch Total RNA Miniprep Kit and converted the RNA into cDNA. Using the Superscript Vilo Mastermix following the manufacturer's instructions, the reaction was performed with PowerUP SYBR Green PCR Master Mix and primers (Table 2) ranging from 50 to 400 nM. Fluorescence was detected using a QuantStudio 6 under standard cycling conditions. Amplification efficiencies were determined using serial cDNA dilutions (Ramakers, Ruijter, Deprez, & Moorman, 2003) and normalized to TBP. Relative expression was calculated using the method described by (Pfaffl, 2001).

	Forward	Reverse
Sox 10	GCCTTACCACTCCTATGACTCC	TCAAAGCTACTCTCAGCCCC
TWIST1	CAATGACATCTAGGTCTCCGGGCCC	TACGCCTTCTCGGTCTGGAGGATG
TFAP2A	CTCCGCCATCCCTATTAACAAG	GACCCGGAACTGAACAGAAGA
PAX3	AAGCCCAAGCAGGTGACAAC	CTCGGATTTCCCAGCTGAAC
CDH1	CCATTCAGTACAACGCCCAACCC	CACAGTCACACACGCTGACCTC
CDH2	TGCGGTACAGTGTAACTGGG	GAAACCGGGCTATCTGCTCG
OCT4	GTGGTCAGCCAACTCGTCA	CCAAAAACCCTGGCACAAACT
Nanog	TGGACACTGGCTGAATCCTTC	CGTTGATTAGGCTCCAACCAT

Table 4. List of primers for rt-qPCR. All primers were obtained from Thermo Fisher.

Atomic Force Microscopy (AFM)

Stiffness values for gels were obtained with a Chiaro Nanoindenter with cantilevers made by OpticsLife11.

An appropriate probe for the stiffness was selected as indicated in the User manual: Chiaro Nanoindenter by Rijnveld, 2015. In this case, a spherical glass tip with radius of 21 µm was used with a spring constant of 0.025 N m^{-1}. To measure the deformation of the cantilever with the polyacrylamide gel, the light of the phase-shift was reflected from the back of cantilever to the sensor. The sample was indented to a depth of 1.5 µm at a velocity of 2 µm s-1. After holding the tip at this depth for 1 second, it was then retracted over a period of 1 second. Measurements were taken from 3 separate points across the diameter of the gel. At each point, Nanoindenter was set to take 3x3 measurements with 50 µm between each measurement. Results were excluded based on factors such as the R-value for line of best fit and overall shape of the curve. Results from the Effective Young's Modulus was selected. 3 biological replicates of the gel were initially tested with 9 technical replicates in each. This was followed by subsequent testing of the gels once a week to determine the stiffness of a specific batch. Any gels that exceeded the proposed stiffness by more than 2-3 fold were automatically discarded.

Immunofluorescence and time-lapse imaging:

All immunofluorescence images were taken at room temperature in a dark room and taken with an upright confocal integrated microscope system (SP8vis, Leica) with a 63× objective.

Time-lapse imaging:

All time-lapse and live-cell imaging was done on a FV1000 Olympus microscope and an EVOS M7000 Imaging system for exactly 24 hours with 5 pictures taken per hour. Compilations of the videos of the time-lapse were recorded at 8 frames per second. Conditions on the microscope mimicked that of the incubator in terms of temperature, humidity and CO2 levels.

Data Analysis:

Cells were monitored individually through ImageJ Manual Tracking plug-in, allowing for manual identification of each cell at every time point. Statistical significance for datasets exhibiting normal distributions was assessed using unpaired Student's t-test (two-tailed, unequal variances) in GraphPad Prism9. Values were represented as means ± standard error of the mean (SEM). The level of statistical significance was set at $P < 0.05$. All P-values were represented as *<0.05 and **<0.005. To assess significance across multiple datasets simultaneously, either a one-way Analysis of Variance (ANOVA) was conducted for normally distributed data or a Kruskal-Wallis test was employed for non-normally distributed data. Unpaired student t-tests were used for any other remaining statistical tests.

Corrected total cell fluorescence (CTCF) is calculated with the following formula:

CTCF= Integrated Density – (Area of cell * Mean fluorescence of background readings)

This was done via ImageJ. Integrated density was done by selecting a cell of interest and selecting ‘Set measurements’ under the Analyze menu. ‘Integrated Density’, ‘Area’ and ‘Mean Gray value’ were then selected, and their values obtained. Each value lines up consecutively with each of the values listed in the formula above.

Chapter 3: Results

Protocol of Neural crest induction of hiPSC

To select the *in vitro* protocol for this system, we must first consider the various protocols that exist. Among the pioneering *in vitro* differentiation protocols is the one crafted by Chambers et al., demonstrating the conversion of embryonic stem cells into NCCs (Chambers et al., 2009). Since then, various protocols have appeared basing much of it on the original paper. Subsequent protocols have drawn inspiration from this seminal work, resulting in a variety of approaches. These methods encompass both swift and gradual protocols, with some achieving differentiation within a matter of days, while others extend the process over weeks. Given our specific interest in examining the EMT effect on the cells, a preference for a more gradual approach is deemed appropriate. In addition, we were interested in a protocol that reproduces the times of development (EMT) observed in vivo. This deliberate choice allows for an extended observational window, facilitating a more thorough understanding of the nuanced EMT process.

Consequently, we opted for a protocol with a total duration of 19 days, as detailed by Kobayashi et al. As depicted in Figure 4A, iPSCs are seeded on day 0 and undergo differentiation to generate Neural Border cells (NBCs). Subsequently, these newly differentiated NBCs are replated and permitted to undergo EMT and finally complete their differentiation to form NCCs on day 19. This timeframe aligns closely with the natural developmental timeline observed in a typical human embryo, which spans approximately 24 days (O'Rahilly & Müller, 1994). Overall, morphologically there is also a significant change over time in the cells. As illustrated in Figure 4B, during the 'NB 0' phase, most cells are

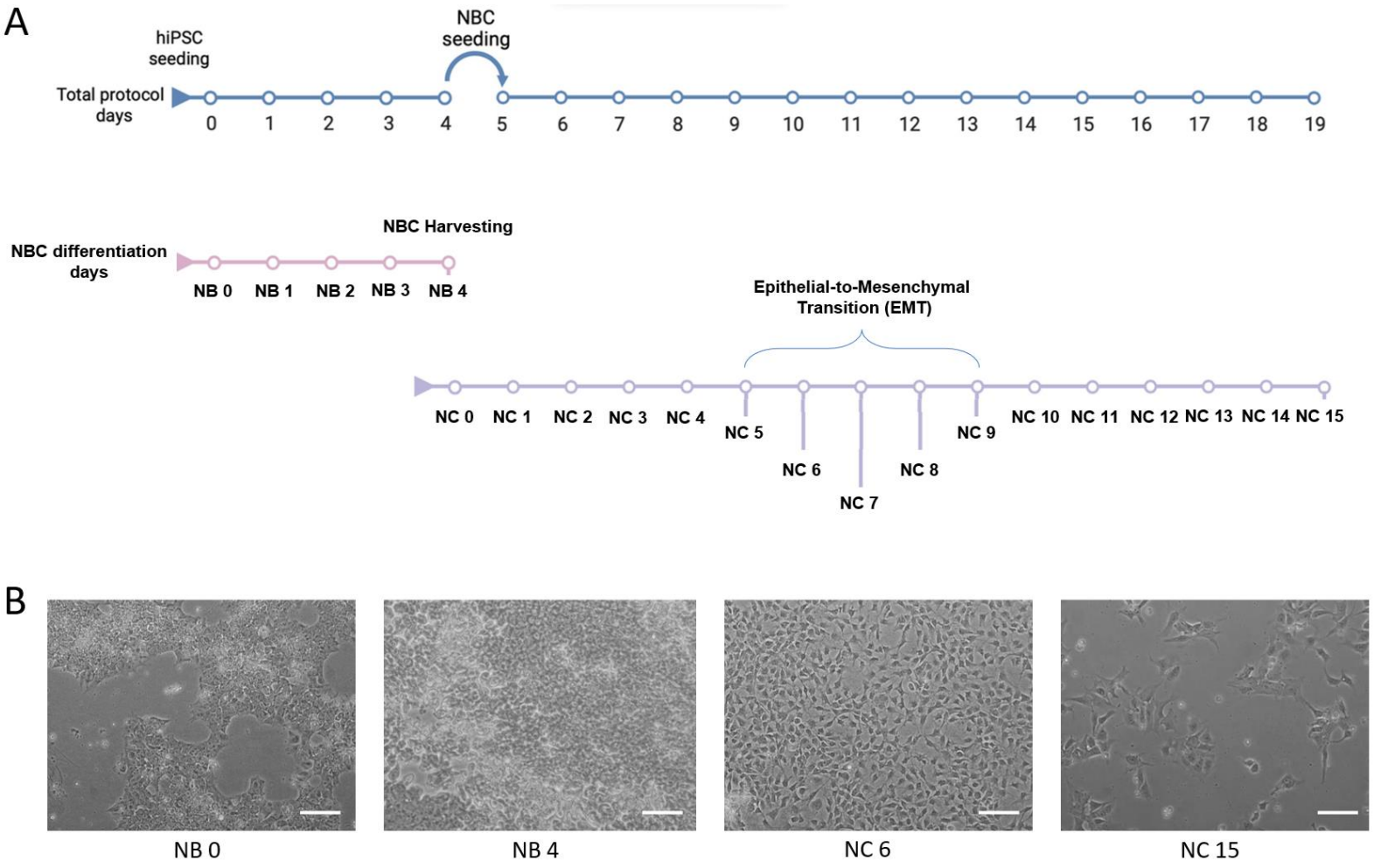

Figure 4. Neural crest induction from iPSC.

A) Timeline of differentiation protocol. All time points for any further figures will be in reference to the 'total protocol days' whereby day 0 is the start of the 2-stage differentiation process and the start of the NBC differentiation stage. Therefore, Day 4 serves as both the final day of differentiation for NBCs but also as the day cells are replated and undergo a second differentiation process towards NCCs. Day 19 is the end of the differentiation protocol resulting in NCC. On Day 4 (NB 4), the cells should be fully formed Neural border cells (NBC). After replating and changing to the final differentiation media, Day 9 (NC 5) to Day 13 (NC 9) should be where we expect to see EMT. (Adapted from Kobayashi et al. 2021).

B) Cells at different stages of the differentiation protocol. Day 0 shows induced pluripotent stem cells (iPSC). Day 4 shows NBC. Day 10 shows cells undergoing EMT. Day 19 shows NCCs. Scale Bar= 50 µm.

clustered, with central regions of these clusters consisting of notably small cells. This is further exacerbated by ‘NB 4’ marking the point where cells transition to a fully epithelial state. At this juncture, many cells are densely packed, covering the entire dish before they are harvested. After a few days of being replated, morphological cell changes become apparent. Even in the 'NC 6' stage, where cells remain quite confluent, distinct changes are observed, with processes beginning to extend from the central cell region and a more prominent nucleus. Subsequently, by 'NC 15', the cells exhibit a substantial increase in coverage area, accompanied by a prominently visible nucleus and numerous processes extending outward.

However, as previously highlighted, these cells typically exhibit the expression of various genes with proteins localized to specific cellular regions. To validate this, cells from three distinct stages of the protocol—'NB 0', 'NB 5', and 'NC 15' (designated as iPSC, NBC, and NCC respectively in Figure 4A)—were selected. RNA was extracted from these cells, converted into cDNA, and subjected to real-time quantitative polymerase chain reaction (qPCR) to quantify RNA transcript levels. This approach allows us to visualize the overall progression of specific RNA transcripts throughout the differentiation protocol. Examining the relative RNA expression in Figure 5A, many values align with what has been documented by Kobayashi et al. from which this protocol has been adapted.

For instance, considering the pluripotency marker *OCT4*, a tenfold decrease is observed by the NBC stage compared to the iPSC stage, and a more than 100-fold decrease relative to the NCC stage. Turning to Neural Plate Border specifiers like *TFAP2A*, there's an initial nearly

1000-fold increase before a slight dip in the NCC stage. Similarly, *PAX3* exhibits a substantial initial fold increase of around 200 before a slight rise to approximately 300. Looking at the Neural crest specifiers such as *SOX10* and *TWIST1*, a notable increase in relative expression is evident. *SOX10* consistently rises, peaking at around 40 times relative expression. In contrast, *TWIST1* maintains relative consistency between the iPSC and NBC stages, experiencing a significant increase only at the NCC stage, roughly comparable to *SOX10*. Finally, examining the cadherins, N-Cadherin (*CDH2*) demonstrates an increasing trend, reinforcing the concept of cells adopting a mesenchymal identity. Conversely, E-Cadherin (*CDH1*) exhibits similar levels between iPSC and NBC stages before undergoing a drastic 1000-fold decrease once the cells undergo Epithelial-to-Mesenchymal Transition (EMT).

While understanding relative gene expression is crucial, multiple steps exist in between the RNA and the final protein. Therefore, it is equally imperative to confirm the actual production of the related protein and its localization. In Figure 5B, cells from the same time points as those in the qPCR analysis were subjected to immunostaining. Notably, E-Cadherin, as depicted in Figure 5A, exhibits high expression in the iPSC and NBC stages, with minimal presence in the NCC stages.

In both the iPSC and NBC stages, most of the staining localizes to the cell membrane and extends outside the nucleus. However, in the NCC stage, faint E-Cadherin staining is observable within the cell nucleus. Intriguingly, Figure 5C' indicates a significantly higher amount of Total Cell Fluorescence (CTCF) in E-Cadherin staining in the NBC stage compared to the iPSC and NCC stages. Yet, when comparing iPSC and NCC stages, there seems to be no discernible difference in CTCF. Furthermore, a greater degree of variance is apparent in the NBC stage compared to the other cell types.

Another antibody used here is *HNK1* which stains for NCCs (Bronner-Fraser, 1987), targets a glycoprotein present on cell membranes (Shih, Schnaar, Gearhart, & Kurman, 1997). Minimal staining is observed in the iPSC stage, while a considerably higher amount is evident in both the NBC and NCC stages, coinciding with the idea of being an NCC marker. This is particularly striking in NCC staining, where nearly every cell exhibits positive *HNK1* expression. This trend is reflected in the CTCF values presented in Figure 5C, with iPSC values notably lower compared to both NBC and NCC. Interestingly, the CTCF values for NBC are almost double those found in NCC, where one might anticipate the highest expression.

Examining the merged images for the immunostains in Figure 5B reveals intriguing features. In iPSCs, *HNK1*-positive cells are mostly individual and excluded from the main cluster, where the majority of cells exhibit a distinctly epithelial character with high E-Cadherin expression. In contrast, the merged images for NBCs display a gradient and mix of cells. Some cells express both E-Cadherin and *HNK1*, indicating a partial-EMT state where characteristics from both ends of the spectrum are exhibited. However, mutually exclusive cells are also evident, with most cells expressing either E-Cadherin or *HNK1* exclusively. Despite the lack of a clearly uniform population of cells, the expression patterns at the three stages are distinct.

Considering the obtained results, encompassing both morphological and genetic aspects, it is evident that these 3 cell populations are distinctly unique from one another. The clear distinction between these cell types supports the notion that the protocol has been accurately followed, establishing a foundation for further experiments.

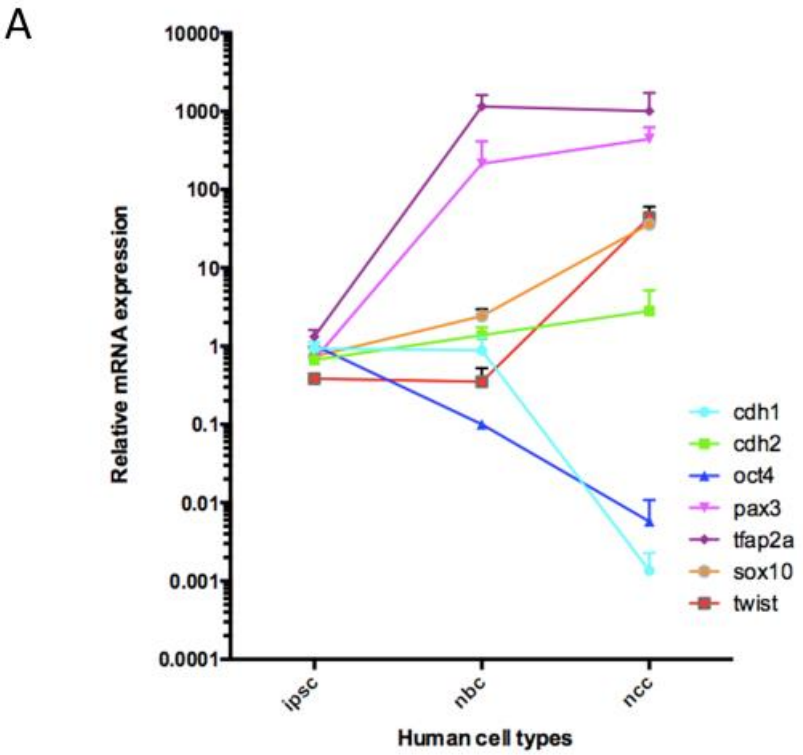

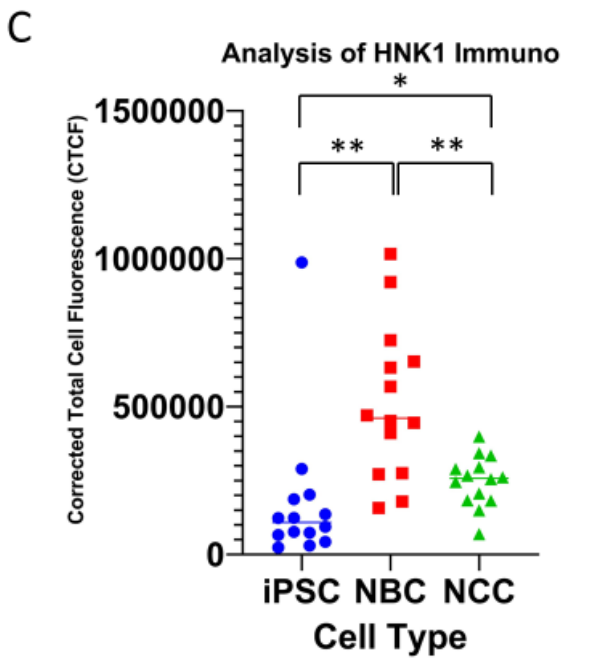

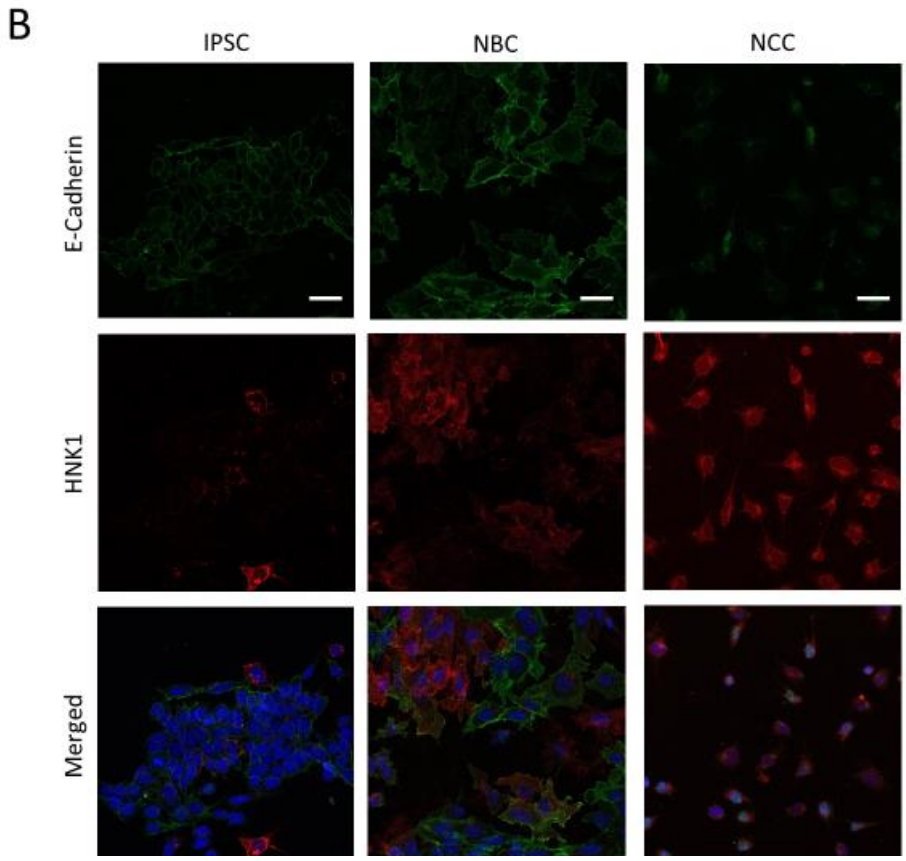

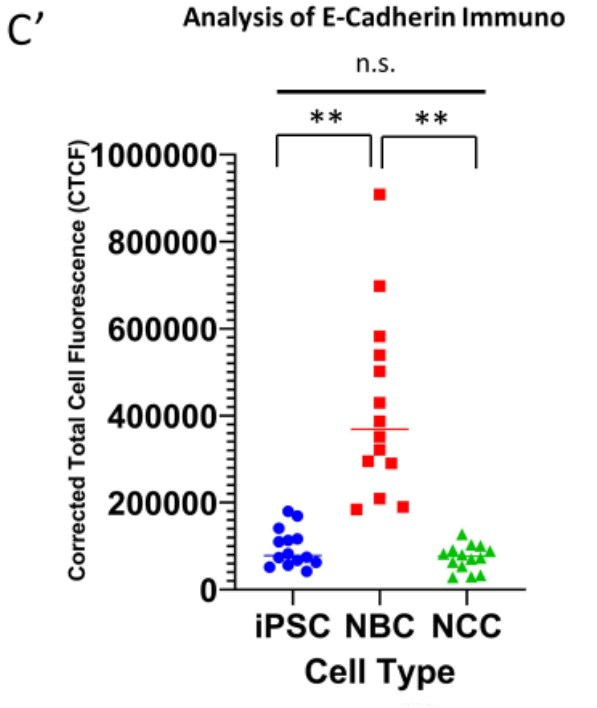

Figure 5. Neural crest Cell induction analysis

A) qPCR of relative mRNA expression levels of various genes of interest. Downregulation of Oct4 showing loss of pluripotency. Upregulation of pax3 and tfap2a shows neural identity (NBC marker). Continuous upregulation of the mesenchymal/NCC markers *SOX10* and Twist from the beginning to the end of the differentiation process. Bars represent mean ± SEM (n = 5 biological replicates used whereby samples were taken from each timepoint).

B) Expression of E-Cadherin (epithelial marker) decreases as EMT occurs. HNK1 is shown to increase as all cells are shown to be marked by Day 19 of the overall differential protocol, confirming the presence of NCCs. It is interesting to note that that despite being an epithelial population, not all cells are marked by E-Cadherin in the Day 5 (NBC) population. Scale Bar= 10 µm.

C and C') Immunofluorescence quantification of HNK1 and E-Cadherin staining. Multiple cells were analysed via ImageJ. C shows significance between all groups suggesting uniquely different HNK1 expression patterns and levels. C' shows that the expression levels of E-Cadherin are significantly different only between NBC and the other two groups; however, when comparing iPSC and NCC expression levels, the difference is not statistically significant. This suggests that NBCs exhibit a more epithelial nature in comparison to the other cell types. Notably, there is variance in the NBC results for both analyses. The bar graph represents the mean (n=14 technical replicates for different fields of view of the same sample). Statistical analysis was done via two-tailed t-test comparing each condition. Line in each represents mean.

Culturing cells on substates of different stiffness: a morphological and cell behaviour analysis

In establishing a suitable substrate for the experiment, a multitude of protocols outlining the creation of substrates with varying stiffness were considered, ranging from Polyacrylamide to Silicone to Agarose gels, each with its own set of advantages and disadvantages. For instance, Agarose gels often possess larger pores than Polyacrylamide gels, potentially raising concerns about cells invading into the gel (J.E. Coligan, 1995). Silicone gels, on the other hand, can be challenging to handle due to the complexity of the material itself.

Among the various options, Polyacrylamide gels were chosen. However, within this category, several protocols exist, such as the need for crosslinking after gel creation to form areas for protein binding (Kumai, Sasagawa, Horie, & Yui, 2021). This step is crucial as an underlying coating of protein or extracellular matrix (ECM) is required for cell attachment. To enable these proteins to attach to the gel, areas for attachment are created through crosslinking. While Sulfo-SAMPA (Shellard & Mayor, 2021) is a commonly used crosslinking agent, the potential toxicity associated with this method led to the adoption of a less toxic alternative, 6-Acrylamidohexanoic acid (AHA) (Labouesse et al., 2021) given the nature of the cells used in the study.

Following the creation of gels, detailed in the Methods section, it was important to ensure both the stiffness values did not differ significantly from the proposed value and the gels exhibited consistency. The Chiaro Nanoindenter is a device that allows us to analyse the overall stiffness of a surface. This is done by analysing the deflection of the cantilever upon hitting the measured surface, as illustrated in Figure 6.

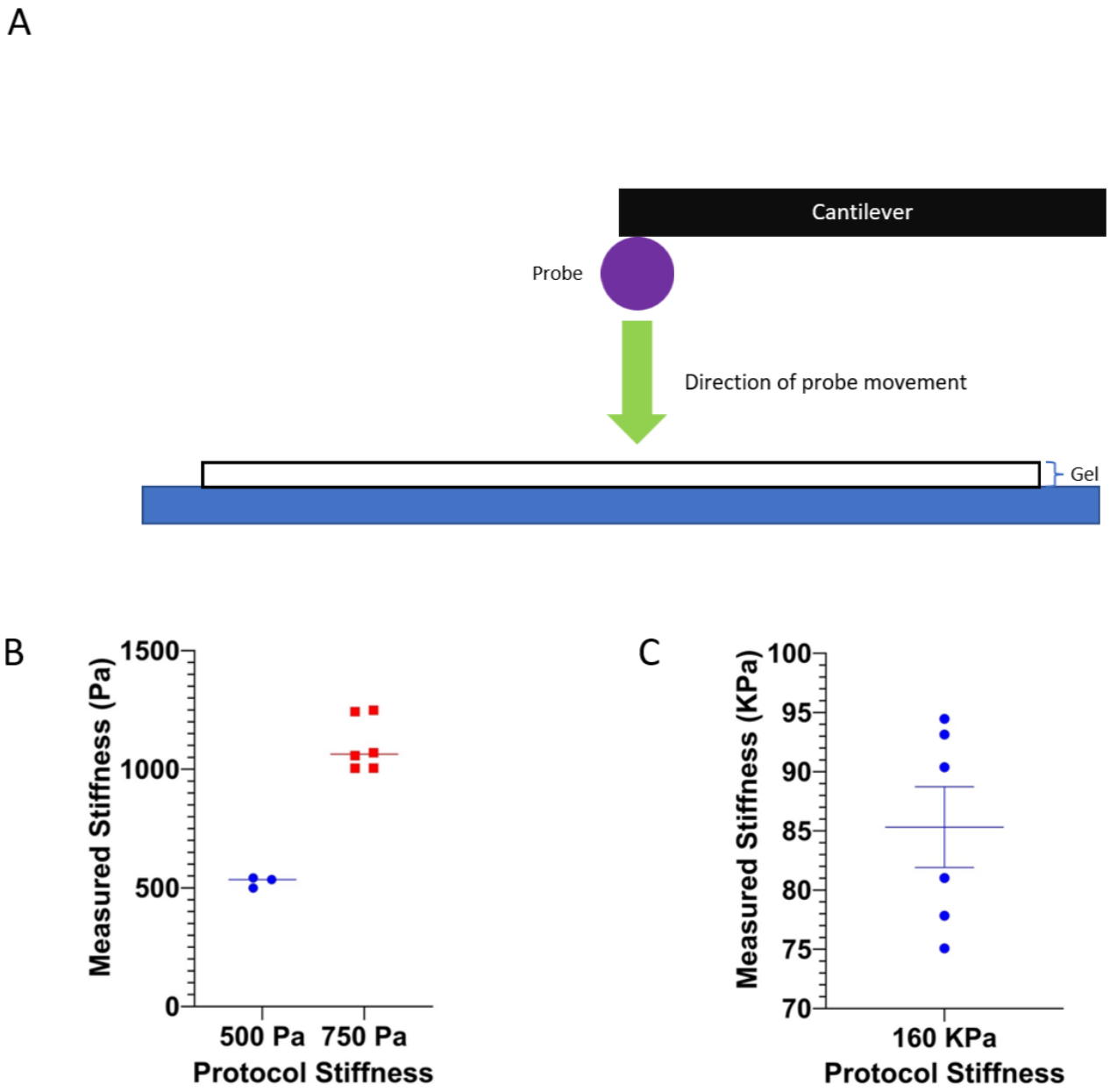

Figure 6. **Gel stiffness measurements.**

A) Graphical representation of gel measurement conducted by the Chiaro instrument.

B-C) Measurement of gel stiffnesses.

Each data point in the graph represents an average calculated from 27 technical replicated were conducted per gel from 6 different gels. Unfortunately, due to soft nature of the gel, the 500Pa gel was often quite difficult to analyse, often leading to no measurements. Notably, the 500 Pa stiffness aligns closely with the Labousse et al. protocol, demonstrating the successful replication of the intended condition. Although the 750 Pa measurement approached 1000 Pa, it remains relatively close to the initial target of 500 Pa. The chart in (C) exhibits higher variability and deviates from the anticipated '160 kPa' value proposed by the original protocol. Despite this, for the sake of consistency, subsequent results will be denoted by the initially proposed stiffness values. The bar through the centre of both graphs represents the mean and the bars on either side in C) represent ± SEM (n = 3 or more biological replicates).

For the experiment, three different gel formulas were deemed necessary: two soft (500 Pa and 750 Pa) and one stiff (160 KPa). The 750 Pa gel served as a control for the 500 Pa, with both results expected to be similar. The 160 KPa gel acted as an overall control for all gels, considering the potential impact of the gel's composition on the results. While the 500 Pa result aligned with expectations from Labousse et al., the 750 Pa result exhibited inconsistency, averaging slightly above 1000 Pa. Similarly, the 160 KPa result not only displayed variance but also differed from the anticipated measurement at ~85.3 KPa. However, the primary objective was to have two soft gels and one stiff gel. Originally the 160 Kpa would be 213~320 times stiffer, however in this case, after the measurement, it appears to be only around 85~170 times stiffer than the current measurements. While this discrepancy is less pronounced than the initial estimate, there remains a substantial difference between the numbers, which is deemed sufficient to proceed with cell plating.

Following the initial cell plating at Day 5 of differentiation, minimal differences are observed in both the 0.5 KPa and plastic conditions, as depicted in Figure 7A. An analysis of the overall cell speed reveals little disparity, indicating that no noticeable alterations have occurred immediately after the cells were plated on the various stiffnesses. Thus, both cell populations seem to maintain a similar profile.

However, a substantial transformation occurs between Day 8 and Day 9, as illustrated in Figure 7A. In the plastic conditions, many cells remain individual, whereas in the 0.5 KPa condition, a considerable number of cells form clusters. Here, a cluster is defined as a group of cells entirely encased by others, maintaining a visible boundary of at least 5 μm on all

sides. Notably, several of these cell clusters in the 0.5 KPa condition increase in size from Day 8 to Day 9, suggesting ongoing cell division, as no discernible change in cell size is observed. Conversely, the plastic condition shows cells with more processes and larger sizes compared to the 0.5 KPa cells. This significant shift is also reflected in cell speed, as shown in Figure 8B. Cells in the plastic condition exhibit higher motility, with the overall average being more than double that of the 0.5 KPa condition. It is intriguing to observe minimal changes in speed for the 0.5 KPa stiffness when comparing Day 5-6 and Day 8-9. Overall, this begins to highlight the difference between cells placed in the 2 different stiffnesses.

Examining the morphological variations across all days for both the plastic and 160 KPa conditions reveals minimal differences in Figure 9. In the initial stages, cells tend to appear grouped with few processes. However, as EMT progresses, there is a noticeable shift toward individualization and increased process formation, aligning with the expected EMT transformation into NCCs observed earlier in Figure 7. The resemblance between both conditions suggests that the gel formula is unlikely to exert a significant morphological impact on the differentiation process.

Similarly, marginal distinctions are noted between the 0.5 and 0.75 KPa conditions. Individual cells observed on Day 5 initiate division, leading to the formation of cell clusters that progressively increase in size. The resemblance between both conditions for both stiffnesses suggests that the gel formula is unlikely to exert a significant morphological impact on the differentiation process.

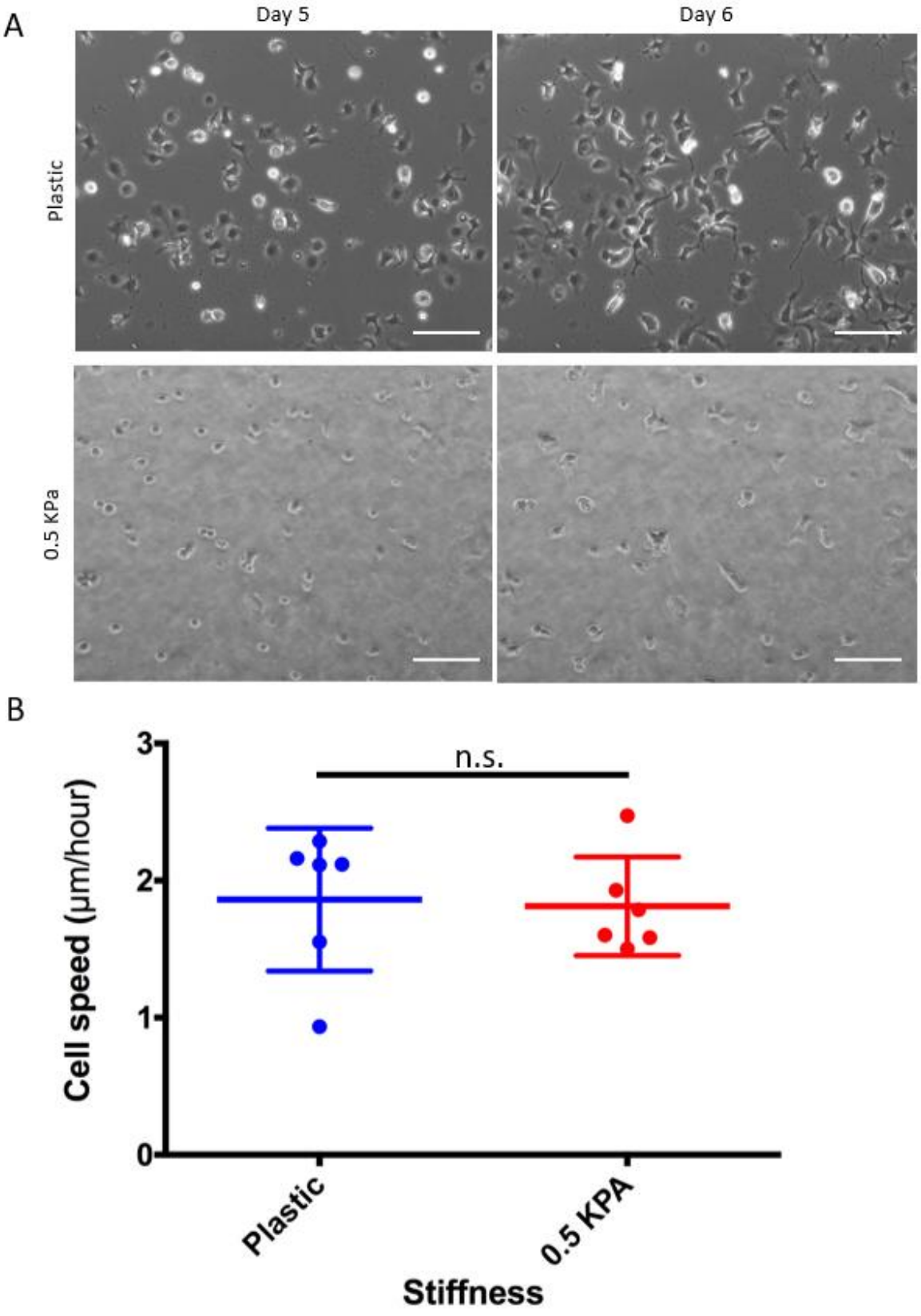

Figure 7. Day 5 to Day 6 cell morphology differences.

A) The first 24 hours of cell tracking shows almost no difference morphologically. Cell number increased from 61 in this FOV to 109. Scale Bar= 25 µm.

B) Analysis of migratory speed showing no detectable difference (p=0.86). Bars represent mean ± SEM (n = 6 biological replicates). Statistical analysis conducted via unpaired student t-test, p=0.563.

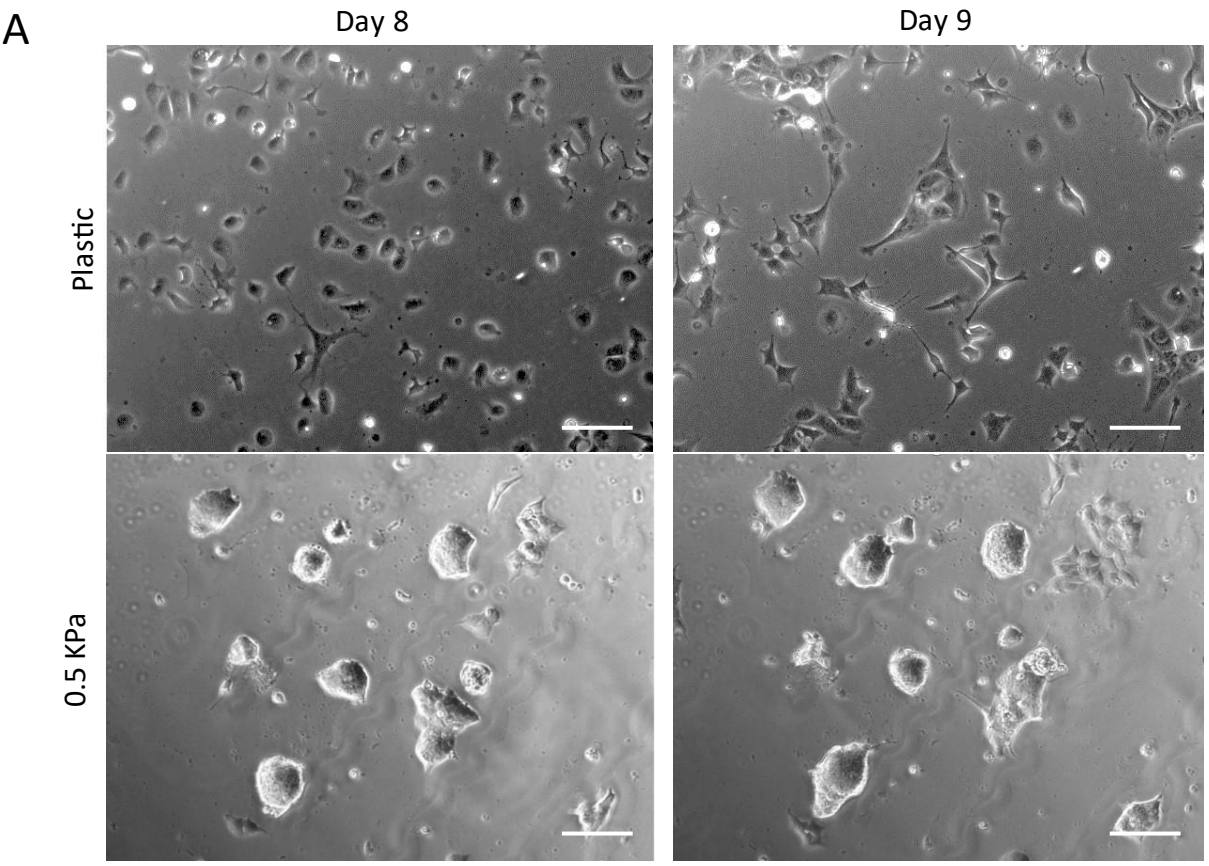

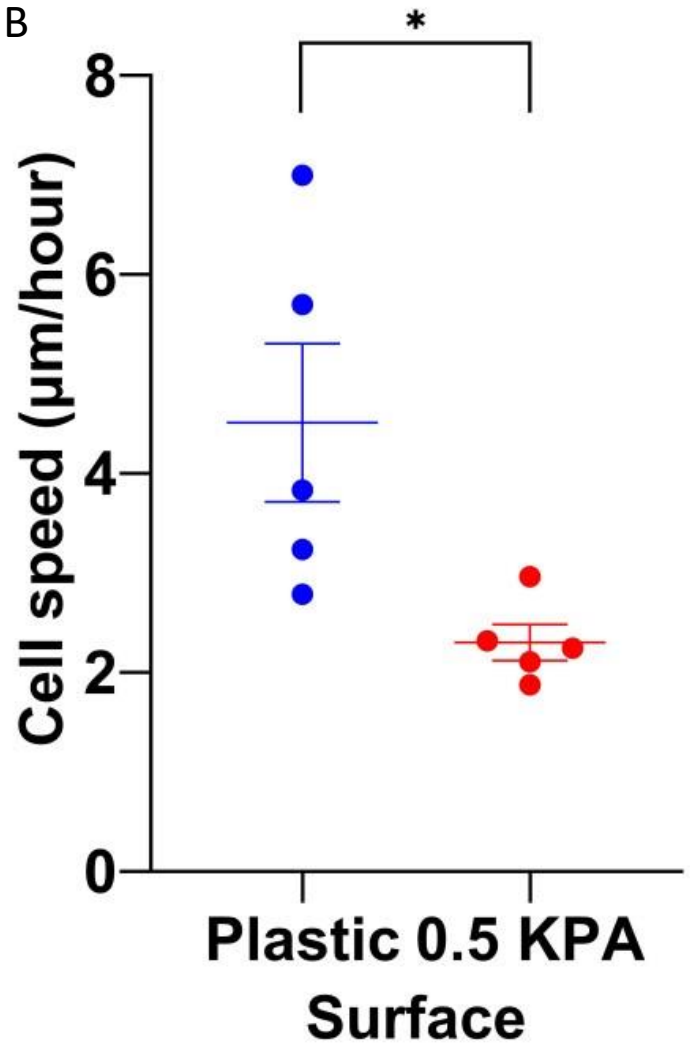

Figure 8. Day 8 to Day 9 cell morphology differences

A) Day 8-9 is where we expect to start seeing EMT with obvious morphological cell differences. Cell number increased from 128 on Day 8 to 181 on Day 9 in plastic and from 266 on Day 8 to 338 on Day 9 in substrate stiffness of 0.5kpa. Scale Bar= 25 µm.

B) Statistical analysis of cell speed (unpaired student t-test, p= 0.02). A large amount of variance is observed in the plastic in comparison to the 0.5 Kpa (n = 5 biological replicates).

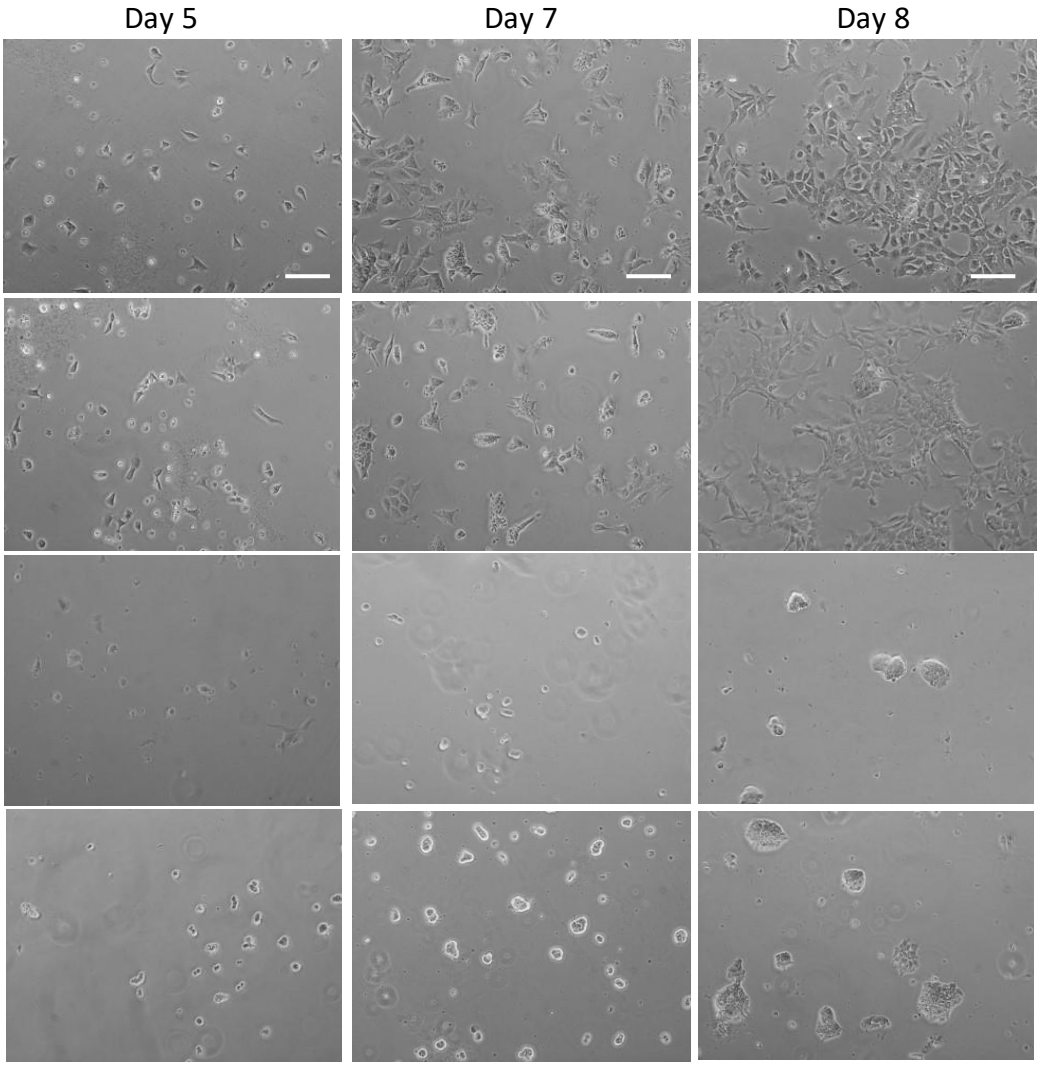

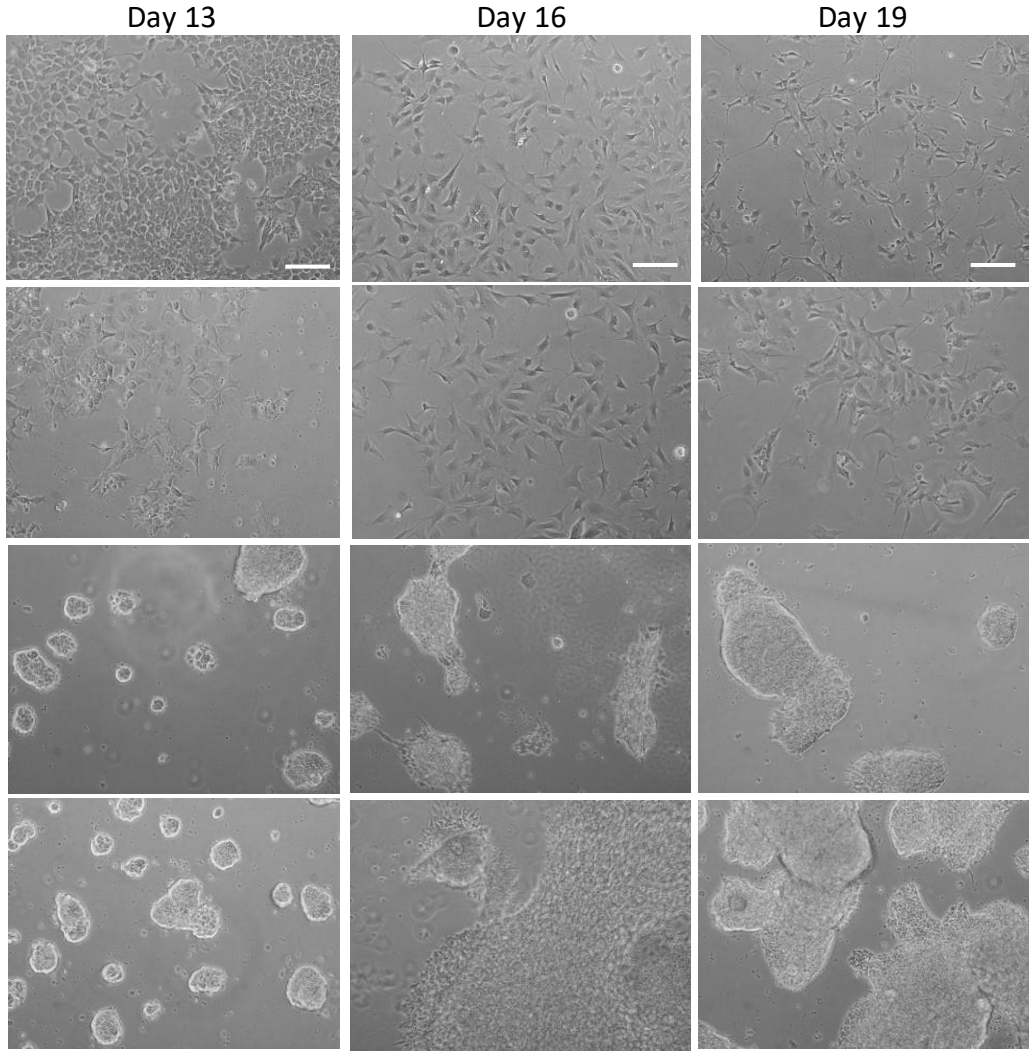

Figure 9. NBC to NCC on different stiffness

Analysing the effect of various stiffnesses on NBC to NCC differentiation process, 0.5 and 0.75kpa has formed huge clusters while in both 160 kpa and plastic, the cells have become far more morphologically mesenchymal. Cell count of this figure was added to 4 other FOVs of the same day and stiffness and shown in Figure 10. Scale Bar= 50 µm.

Conversely, when comparing the stiffer (160 KPa and plastic) and soft conditions (0.5 KPa and 0.75 KPa), a substantial difference emerges after Day 5. Beyond the earlier noted distinctions, this contrast intensifies from Day 13 onwards, with many clusters growing to sizes exceeding the field of view (FOV). Particularly from Day 16 onwards, numerous clusters reach sizes challenging to quantify due to their scale.

Much of the morphological data is reflected in the analysis as shown in Figure 10. It is important to note that much of this analysis does hinge on the idea of having clusters present to analyse in the first place. For example, little to no clusters exist in the initial plating of cells across all stiffnesses. However, with the progression of time, clusters start to enlarge in the soft conditions, while seemingly diminishing in the stiffer conditions, as illustrated in Figure 10A. As the differentiation protocol approaches the final days, the number of clusters for high stiffness becomes exceedingly sparse as they transform into NCCs. Conversely, a different issue arises for cells in the soft conditions, where the clusters grow to an overwhelming size, causing many to merge and necessitate multiple FOV assessments. For simplicity, the analysis was conducted on only single FOVs, indicating that the results Day 19 are underestimated with the true diameter most likely being much greater. Nonetheless, the value indicated for the diameter is notably larger in both the soft conditions compared to the stiff conditions.

Likewise, the cell numbers within the clusters exhibit a progressive increase over time, as illustrated in Figure 10B. While minimal change is observed in the stiffer conditions, the cells in the soft conditions demonstrate an almost exponential growth over time. Overall, this begins to suggest that the cells of the stiffer conditions are most likely fully mesenchymal and are fully differentiated NCC. However, the cells in the soft conditions, are so

morphologically distinct that it is not known whether they are epithelial, mesenchymal or have undergone partial-EMT, requiring classification. To assess whether cells in the soft conditions maintain a mesenchymal morphological behaviour, clusters from Day 18 at 0.5 KPa were transplanted and observed for 24 hours as shown in Figure 11. Initially, at 0 hours, minimal differences were observed between the clusters. However, at 12 and 24 hours, the transplant of 0.5 KPa to 0.5 KPa showed little to no change in cell behaviour. In contrast, the cluster plated on plastic exhibited significant changes. By 12 hours, many cells had migrated away from the central mass, displaying multiple processes. This migration and expansion continued until 24 hours, with the area of cell expansion widening, and the cells exhibiting neuronal-like processes. While the cells likely retained mesenchymal properties as a cell cluster, the underlying stiffness may have been too low for proper EMT, resulting in a behavioural arrest. Complete differentiation might occur only after altering the underlying stiffness.

These experiments conclusively demonstrate that substrate stiffness significantly influences cell behaviour. A remarkably low stiffness tends to induce a more epithelial-like behaviour, whereas a higher stiffness prompts a shift toward a more mesenchymal phenotype. Although transitioning cells from low to high stiffness can rescue the clustering effect, the identity of cells at low stiffness—whether epithelial, mesenchymal, or neither—remains uncertain. The rapid initiation of migration and process formation (Figure 11), typically a gradual process according to the original protocol, suggests that these cells might be primed toward a mesenchymal state. Consequently, further in-depth analysis is warranted to understand their precise nature.

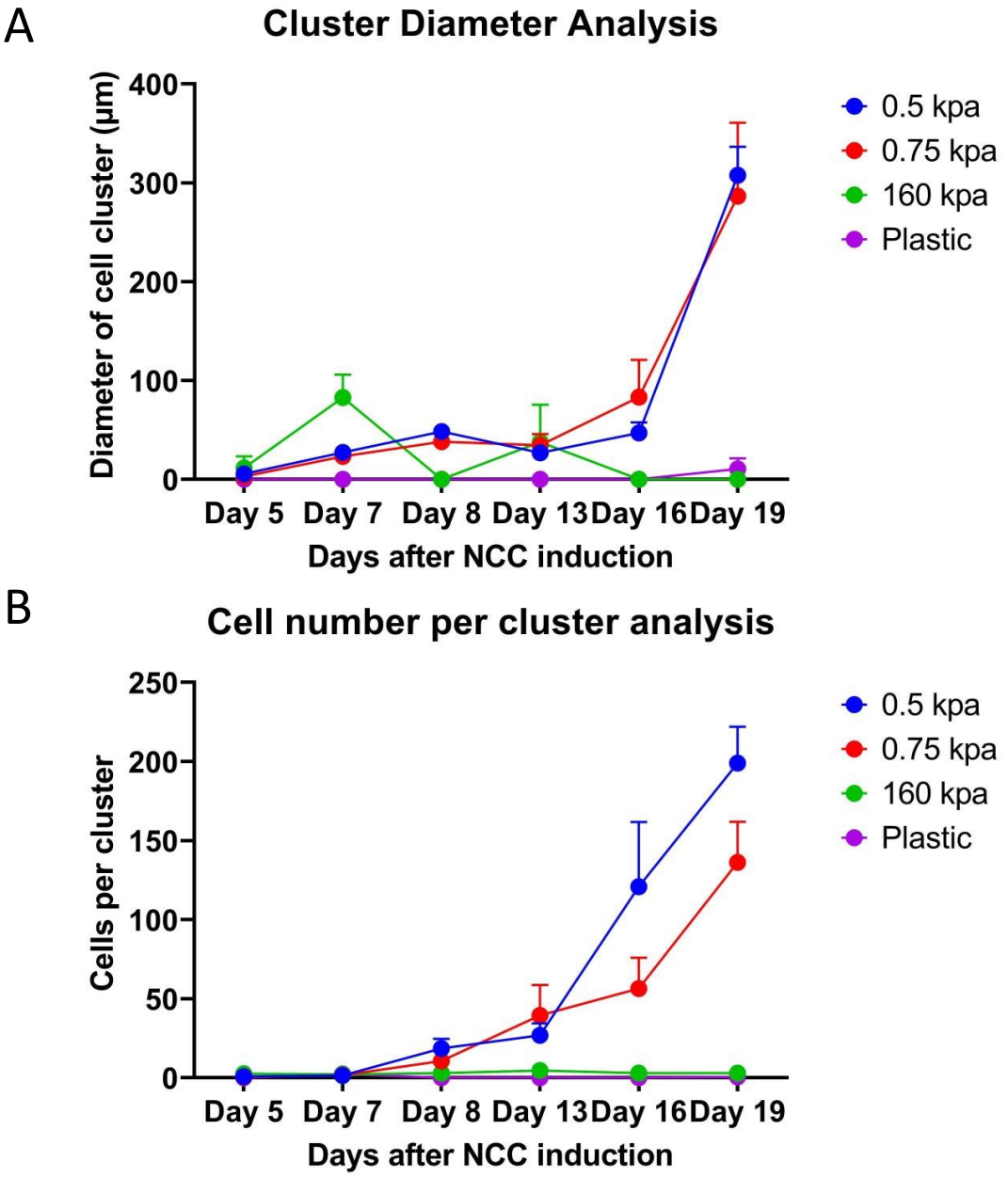

Figure 10. Cluster size and cell number increase over time.

Through the analysis of the clusters observed in Figure 8, an increase in both cluster size and cell number is observed. Clusters are defined by cells entirely encased by other cells, but also maintaining a clear visible boundary of at least 5 µm on all sides. Cells are counted as being in a cluster if they fulfil the above requirements. It is important to note that monitoring the number of clusters does become a limiting factor in this analysis. Bars represent mean ± SEM (n = 5 biological replicates).

A) An overall increase in cluster diameter is observed in soft conditions (0.5 Kpa and 0.75 KPA) while this decreases in stiff conditions (160 Kpa and plastic). This potentially means that the cells on soft conditions are retaining or maintaining epithelial-like properties while the cells in the stiff conditions is becoming more mesenchymal.

B) A similar increase is noted in the number of cells per cluster in the soft conditions versus the stiff conditions. This leads to an increase in cell number in soft conditions since the overall cell sizes are not increasing. Little to no difference is observed in the stiff conditions due to both the lack of clusters, but also the fact that most cells have become mesenchymal.

Culturing cells on substates of different stiffness: a molecular analysis

To further characterize these clusters and understand their properties, it is important to assess the expression of key mesenchymal and epithelial markers, as established in earlier experiments. Examining the epithelial characteristics of these clusters involved employing immunostaining against E-Cadherin, as depicted in Figure 12 A. As previously highlighted, E-Cadherin serves as a crucial marker for epithelial cells. The cells from the Plastic condition on Day 19 exhibit minimal to no E-Cadherin staining. Conversely, the 0.5 KPa cells display substantial E-Cadherin staining, particularly around the cell membrane. These findings are corroborated by the analysis in Figure 12B, indicating no significance in the DAPI values between both conditions. However, substantial differences in CTCF for E-Cadherin staining are evident, with a significantly higher amount observed in the 0.5 KPa condition. This suggests the retention of epithelial-like properties in the cell clusters.

An RT-qPCR was also conducted for the cells across different conditions (Figure 13). The RNA transcripts for *CDH1* (E-Cadherin) exhibit the highest levels in NBC cells and the lowest in the hard (plastic) or 160 KPa conditions (Figure 13A). The two soft conditions both fall almost in between the plastic and NBC levels, forming a gradual gradient. Conversely, when examining *CDH2* (N-Cadherin) levels, a higher expression is observed in all other conditions compared to the NBC level, with the softer condition appearing to have the highest expression. However, it's crucial to note that the differences in *CDH2* levels between the conditions are not statistically significant. The results for these cells seem to be ambiguous, suggesting a potential reversion to a previous

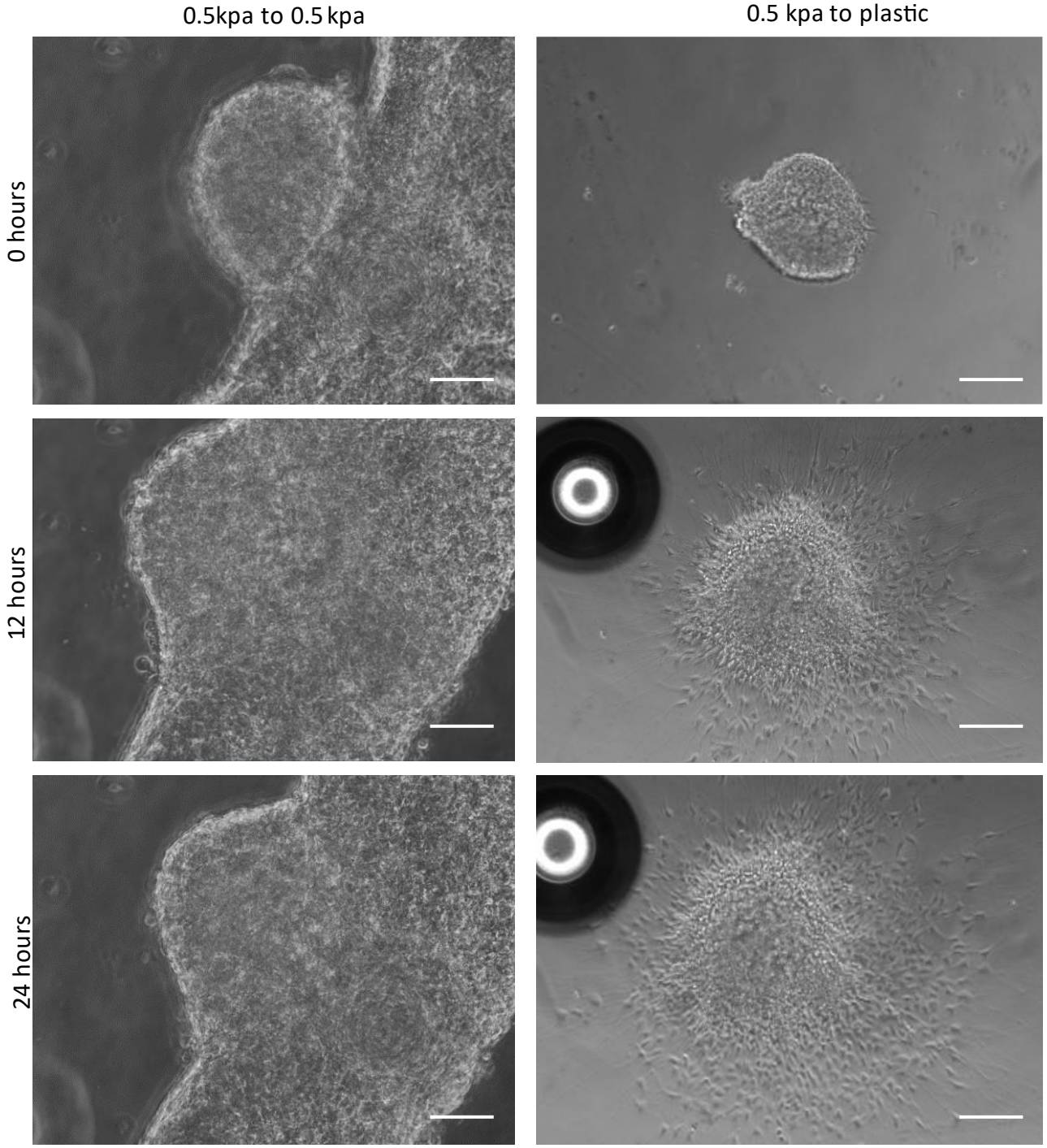

Figure 11. 0.5 Kpa cell cluster transplant to a higher stiffness
Transplant of a cell cluster from 0.5kpa to both 0.5kpa and plastic. Little effect is shown in the cell behaviour after 24 hours when moving them between the same stiffness. However, when moved to a higher stiffness, the cells readily attach and migrate very rapidly within the first 12 hours with far less obvious spreading after 24 hours. Scale Bar= 25 µm.

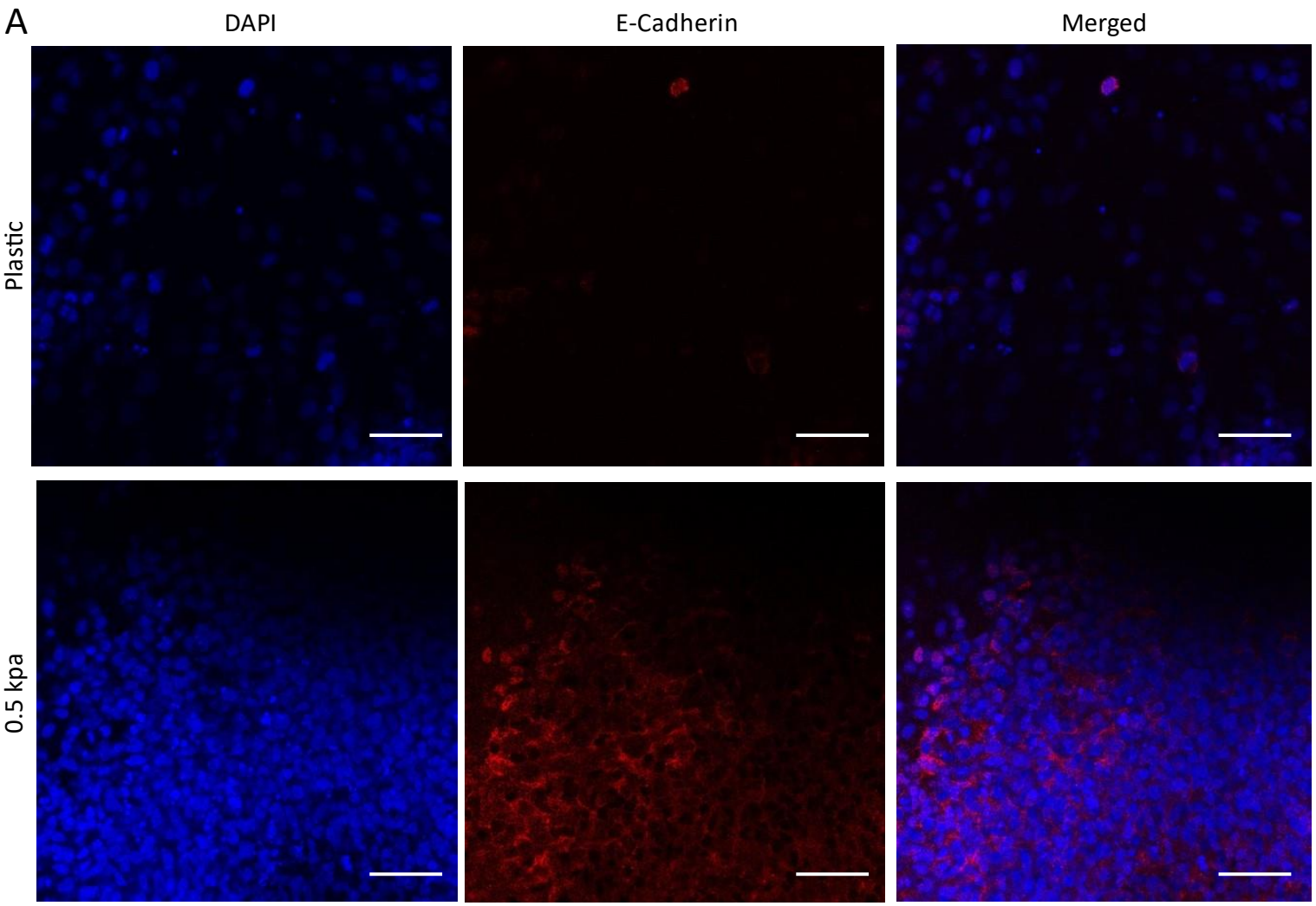

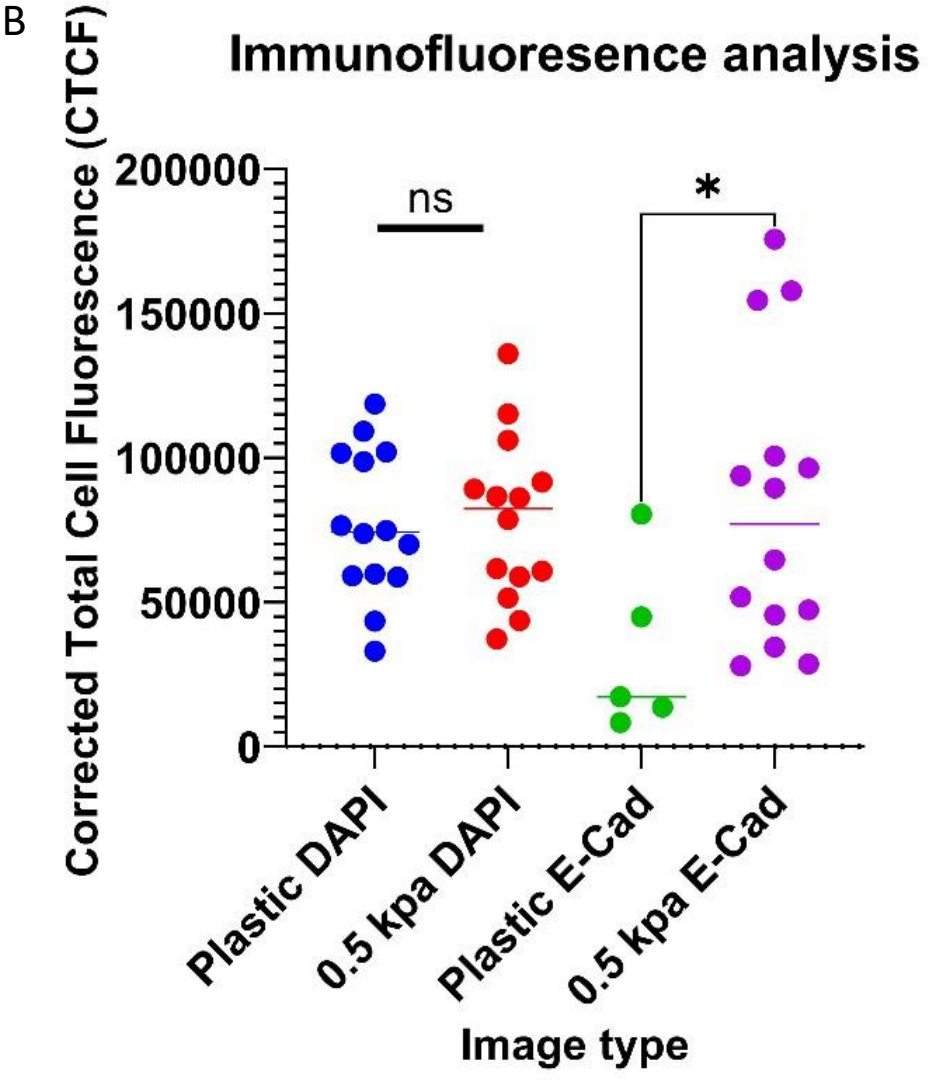

Figure 12. 0.5 KPA cluster Immunofluorescence and analysis

A) Immunostaining of cell clusters in 0.5kpa and groups of cells in plastic. Much higher expression of E-Cadherin can be seen in the low stiffness instead of high implying potential retention of Epithelial state. Scale Bar= 10 µm.

B) Statistical analysis of DAPI exhibits no significant difference, as anticipated for a control. However, in the comparison between E-Cadherin and plastic conditions, plastic shows a significant decrease, indicating a potential loss of epithelial properties. Contrastingly, the notably high CTCF value observed in the 0.5 KPa condition suggests that these cells may still retain epithelial characteristics. CTCF calculation explained in Methods. Bar through the centre of each set of results represents mean (n = 5 biological replicates minimum).

cell state, considering that iPSCs are not strictly classified as either epithelial or mesenchymal.

To assess whether cells on different stiffnesses have reverted to iPSCs, pluripotency markers NANOG and *OCT4* were tested. iPSCs displayed the highest relative expression in Figure 13B, followed closely by NBCs. As all other stiffness conditions showed lower expression than iPSCs and NBCs, it is unlikely that the cells reverted or retained their NBC state. Notably, the 0.5 KPa condition exhibited similar NANOG expression levels to NBCs, suggesting a potential retention rather than reversion. To further explore this, we evaluated Neural Plate Border specifiers *PAX3* and *TFAP2A* (Figure 13C). All substrate stiffness conditions demonstrated higher expression in both *PAX3* and *TFAP2A*, indicating that the expression levels in the soft conditions more closely resembled those in the stiff conditions. This makes it unlikely that the cells retained their NBC state.

To investigate whether there might be an issue with the expression levels of neural crest specifiers preventing EMT, we examined *SOX10* and *TWIST1* (Figure 13D). *SOX10* showed the highest expression in the stiff conditions, with 0.75 and 0.5 KPa conditions falling slightly below but still surpassing NBCs. *TWIST1*, while exhibiting similar expression levels between the two stiff conditions and two soft conditions, displayed a statistically significant difference between the Hard and 0.75 KPa conditions. This decrease in *TWIST1* implies a lower-than-expected level of neural crest specifiers, potentially reducing the likelihood of undergoing EMT.

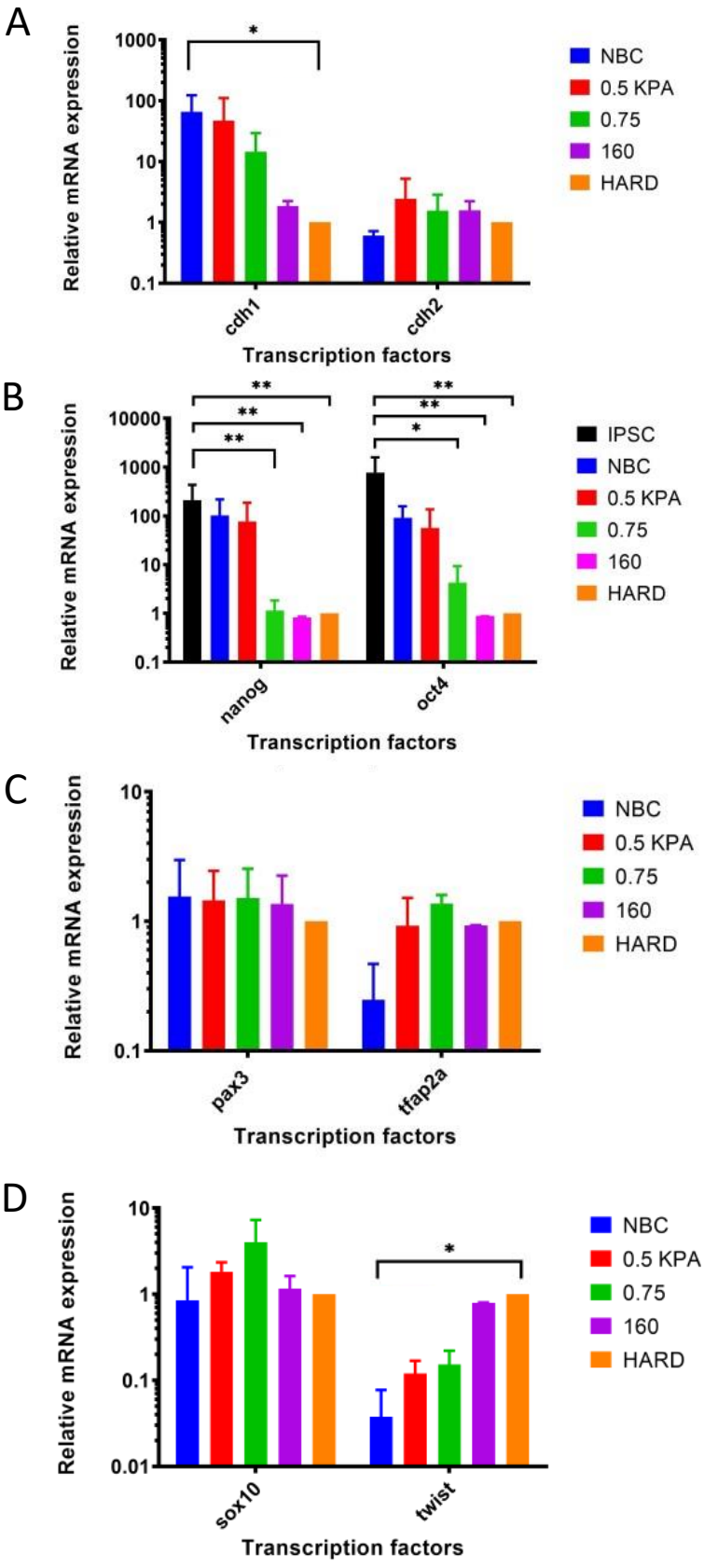

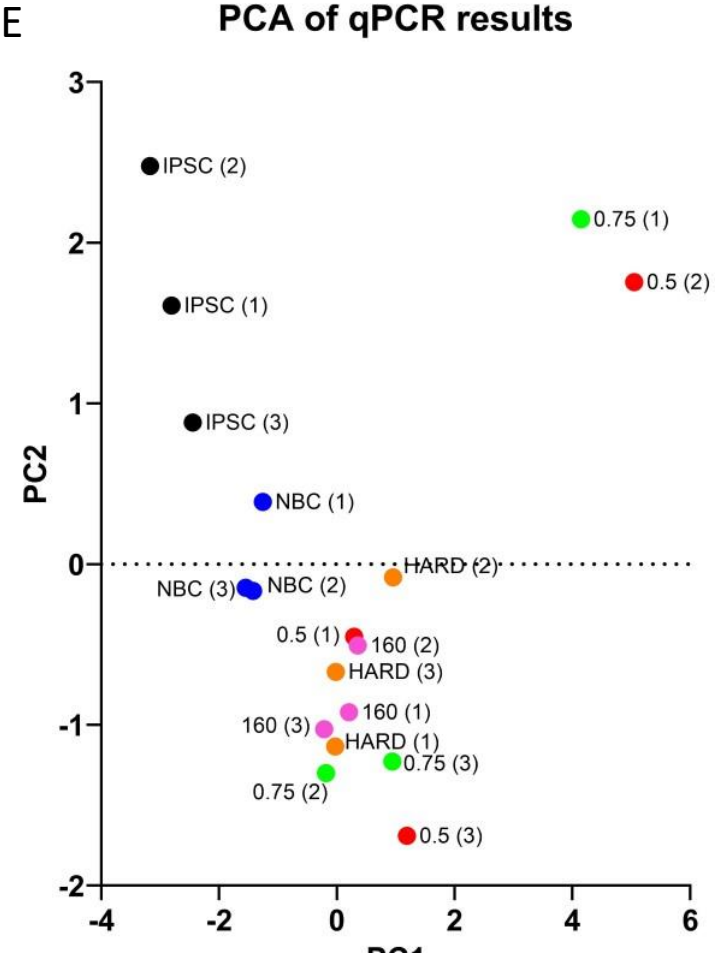

Figure 13. qPCR analysis of cells.

Only significance in figures is shown. Any comparisons made between any other cell types/gel stiffnesses were not significant (n.s.). All statistical tests were done via one-way analysis of variance (ANOVA, Kruskal-Wallis test). All individual tests between stiffnesses of the same gene was done via Students T-test.

A) qPCR analysis of the cells at various stiffnesses show that CDH1 (RNA of E-Cadherin) is more highly expressed in the lower stiffness and NBC in comparison to the higher stiffnesses (p=0.01). Little difference is seen between the different conditions of CDH2 (RNA of N-Cadherin) (p=0.46).

B) To discount the possibility of cells reverting to a previous cell state i.e IPSC, transcripts of NANOG (p=0.0028) and OCT4 (p=0.0018) were analysed. Both showed significant difference between the iPSC and the other cells, ruling out that possibility.

C) qPCR analysis of the Neural plate border specifiers, PAX3 (p=0.09) and TFAP2A (p=0.09) show some difference between NBC and the cells further down in differentiation. Bars represent mean ± SEM (n = 3 biological replicates).

D) qPCR analysis of the cells for Neural crest specifier and EMT marker show little difference for SOX10 (p=0.95) while Twist (0.0092) shows significantly higher expression between the NBC, low and high stiffness. This also the only significant value (p=0.011) between the stiffness conditions of hard and 0.75 kpa. Bars represent mean ± SEM (n = 3 biological replicates).

E) Principal component analysis (PCA) of the qPCR data. iPSC and NBC form a small distinct section of the graph, however the cells on the different stiffnesses are not separated clearly and are mostly all clustered together.

To condense and visually represent the RT-qPCR data effectively, we employed Principal Component Analysis (PCA). PCA is a technique that transforms correlated variables into principal components, capturing the maximum variance in the data. This transformation simplifies data complexity while retaining crucial information, revealing underlying patterns and structures, and enhancing interpretability (Jolliffe, 2014). Figure 13E summarizes the data, showcasing distinct clusters. iPSC data forms a small, isolated cluster in the upper left corner, while NBCs constitute another group just below. The 160 KPa and hard conditions also form a unique cluster. Notably, the 0.5 and 0.75 KPa results surround these clusters, almost creating a ring around the high stiffness results. It's essential to acknowledge that PCA is typically applied with a more extensive set of genes and samples, producing clearer and more uniform clusters. Additionally, any inherent errors in the results are magnified by PCA due to the data available for analysis thus far. Nonetheless, these results suggest that the low stiffness results are not that different from the high stiffness values implying high similarity. This also shows that transcriptionally the NCCs on either stiff or soft gels are not that different and perhaps it may be another factor or genetic pathway, unaddressed here, that may be responsible for this difference.

Chapter 4: Summary and Discussion

Summary

The objective of this project was to establish a robust system for investigating the influence of substrate stiffness on EMT. To attain this objective, two pivotal requirements were recognized: the necessity for cells consistently undergoing EMT and the creation of a reproducible substrate. NBCs, transitioning into NCCs through EMT, were chosen for this investigation. An established protocol was implemented to induce EMT and subsequent differentiation in these cells. Following this, cells from three distinct timepoints—representing iPSCs, NBCs, and NCCs—underwent comprehensive analysis encompassing morphological evaluations, transcriptional studies, and immunostaining techniques. Only once reproducible data that mirrored and showed consistency with existing knowledge, did the project proceed. Likewise, a proven protocol renowned for generating substrates with reliable stiffness was selected and rigorously validated. While not every stiffness value precisely matched the original protocol, the closeness deemed them acceptable.

With the established gel and cell differentiation protocols, it then became imperative to combine the two to study whether it constituted a robust system. Our stiffness levels—0.5 KPa, 0.75 KPa, 160 KPa, and plastic—were employed for comprehensive assessments, involving morphological evaluations, transcriptional studies, and immunostaining techniques. Initially, no morphological disparities were evident across all stiffness levels. However, as time advanced, two distinctive phenotypes emerged. Lower stiffness conditions prompted cells to group and form clusters, indicative of an epithelial-like state, while higher stiffness conditions facilitated EMT, resulting in a mesenchymal phenotype.

Subsequent analysis revealed that cell clusters in lower stiffness conditions increased both in cell number and size. Their behaviour, characterized by a lack of overall cell movement speed and distinct cell processes, suggested an epithelial nature. Immunostaining corroborated this, showing elevated E-Cadherin expression in these clusters.

Despite assumptions that cells on a soft substrate might lose mesenchymal properties, transplantation of the 0.5 KPa cluster contradicted this, suggesting these cells were primed for EMT. RT-qPCR data indicated lower overall E-Cadherin levels compared to NBCs. Likewise, the expression levels of neural plate border specifiers such as *PAX3* and *TFAP2A* are comparable to that of the NCCs, overall being higher than NBCs. Neural crest specifiers (*SOX10* and *TWIST1*) exhibited higher expression in soft conditions compared to NBCs but not reaching NCC levels. This partial inhibition of mesenchymal properties implies that changes in substrate stiffness may affect specific factors in the overall EMT process.

Discussion

Throughout the project, three main aims were created and each with their own points of contention. Commencing with the evaluation of the *in vitro* cell protocol, the protocol was largely successful, namely the morphological section of the differentiation protocol showed clear changes in cell size and shape, characteristic of EMT. However, certain RT- qPCR results differed from expectations. Specifically, in the adapted protocol from Kobayashi et al., where *TFAP2A* expression was anticipated to remain relatively constant between NBC and NCC stages, Figure 6 illustrates an increase. It's crucial to consider the variance in sample sizes; while this report utilized five repeats, the referenced paper employed three. This disparity could account for the nuanced differences observed in the RT-qPCR results.

Nonetheless, this does not account for the immunostaining results observed in Figure 6B. Notably, both the E-Cadherin staining and *HNK1* exhibit certain irregularities. For instance, E-Cadherin is detected in the nucleus of NCC when its expression is expected to localise to the cell membrane. Although not reported in NCCs, there have been previous papers noting the effect of E-Cadherin as a potential transcriptional regulator (Du et al., 2014; Soncin et al., 2011). The variable levels of E-Cadherin staining in the nucleus, as evident in Figure 6B, suggest a plausible role in the transcriptional regulation of factors like *TWIST1*. Although limited, there's existing evidence supporting this notion (Soncin et al., 2011).

Similarly, there's a notable presence of *HNK1* expression in the nucleus, despite it being a known membrane glycoprotein. This might be explained by the synthesis of the protein component of *HNK1* within the cell, considering the protocol designates these as newly fated NCCs. Figure 5B also reveals limited overlap with DAPI (nuclear staining), with much of *HNK1* localizing near the proposed nucleus, indicating potential production in the rough Endoplasmic Reticulum (ER) and transportation to the cell membrane which has been previously shown as shown by Jiang et al., 2009.

However, this does not account for the fact that *HNK1* is also shown to be expressed in the NBCs. This could be attributed to a non-homogeneous cell population resulting from the differentiation protocol. Even in iPSCs in Figure 5B, there are outliers expressing *HNK1*, suggesting potential proliferation and differentiation, potentially influencing neighbouring cells. This factor is crucial when aiming for a relatively pure epithelial population to study EMT. Despite this, the overall number of E-Cadherin-expressing cells significantly outweighs the *HNK1*-positive cells. The fluorescence data is also showing a large amount of variance at

the NBC across both Figures 6C and 6C', lending itself to the idea that the cells are extremely likely to be in a non-homogenous population. This is important to keep in mind when plating these NBCs onto varying stiffnesses.

Following the plating of cells onto various stiffness substrates, although not explicitly shown, cell survivability emerges as a notable concern on low stiffness surfaces. As a result, many of these cells end up dying off leading to diminished cell populations. This raises inquiries into the survival mechanisms of specific cell types. As earlier highlighted, epithelial cells, reliant on cell-cell adhesion and related factors, may face challenges in survival if cell numbers are severely diminished. Thus, surviving cells might inherently possess mesenchymal characteristics or have undergone partial EMT. These cells, constrained in their mobility due to gel limitations, could tend to aggregate, forming distinct clusters. This hypothesis gains some support from various observations. For instance, in the Day 19 cells depicted in Figure 9, plastic conditions exhibit cells with unusually extended processes resembling neuronal axons. If the NBCs already harbor a subpopulation that has undergone EMT, by Day 19, some might progress further in the differentiation process, potentially giving rise to neural progenitors. Additionally, in the explant experiment (Figure 11), akin to mesenchymal cells, neuronal processes are evident outside the main cluster, especially in the transition from 0.5 KPa to plastic. This hints at substrate stiffness potentially acting as a selective pressure, favouring specific cell types for survival. This selective pressure concept could also offer insights into the varying RNA expression levels observed in the RT-qPCR data (Figure 13). However, this notion faces challenges, particularly in explaining the sustained high expression of neural plate border specifiers, *PAX3* and *TFAP2A*, in soft conditions. If cells

were further along in differentiation, these factors should ideally exhibit lower expression in softer conditions.

Although stiffness may be affecting EMT, there are also simpler explanations for this potential behaviour. Throughout this project, issues often occurred with the softest gels, in the creation of the gels to the attachment of cells to the respective gels. When cells are cultured on soft substrates, there is often changes in cell behaviour when compared to cells cultured in stiffer substrates (Saha et al., 2010). As a result, it wouldn't be too absurd to have alterations in the changes to cell-substrate adhesion and cell-cell adhesion. Normally, cell-substrate adhesion and cell-cell adhesion often requires a variety of various mechanisms and junctions (desmosomal, gap, tight, etc) (Gumbiner, 1996) to attach to both the underlying surface and each other. However, due to soft surfaces, cells may not readily attach leading to a more ball like appearance as previously reported (Saha et al., 2010). Lower rates of cell survival have also been reported in cells that lose their attachment (Frisch & Francis, 1994) which was generally observed during this experiment. Therefore, what could potentially be occurring is an artificial selection for cells that are able to survive by attaching to each other. This is observed in Figure 9 where the clusters simply grow and show no mesenchymal cell characteristics despite having factors present that clearly express mesenchymal properties in stiffer conditions. Furthermore, as the clusters begin to grow, their weight may begin bearing down on the softer gels. Due to the softness of the gel, this creates 'pits' in the gel. The compressive force generated by cells on the 'surface' of the clusters then leads to pressure being exerted on the cells below, again further changing the cells. At the same time, this pressure could also artificially be generating a stiffer surface allowing for further changes in cell behaviour. It is important to note that many of these suggestions are possible, however, without further characterisation of these cells outside of

phase contrast microscopy, it is difficult to ascertain their validity. Similarly, many of the changes in both the gel and cells at various stages must also be mechanically analysed to understand their exact properties.

An alternative hypothesis suggests that substrate stiffness might be instigating molecular changes, resulting in an 'apparent' EMT. This idea proposes that, in a way, all cells in the clusters by Day 19 are poised and prepared to undergo EMT, albeit slightly inhibited due to the low stiffness. Notably, cells in 0.5 KPa maintain consistent speed from initial plating to the presumed end of EMT, indicating the retention of epithelial-like properties within the cluster. The transplant experiment in Figure 11 further supports this notion. When cells from a low stiffness is placed in a high stiffness setting, extensive cell migration occurs within 12 hours, implying a rapid EMT response. This contrasts the 5-day EMT period indicated in the Figure 5A protocol, suggesting that many mesenchymal phenotypes were already primed and required increased stiffness to complete EMT. This idea is also further supported by the RT-qPCR data with many graphs of the cells in low stiffness being partially in between the NBC and stiff conditions.

Furthermore, this hypothesis is more strongly supported by the RT-qPCR data in combination with the immunostaining data. For example, in Figure 12, there is clear E-Cadherin expression in a cluster on the 0.5 KPa surface suggesting an epithelial like nature. Similarly, when looking at the RT-qPCR data, E-Cadherin is shown to be higher than the stiff conditions but far lower than the NBCs. Likewise, an increased expression of N-Cadherin in low stiffness cells suggests that the cells are 'more' mesenchymal than the cells in stiff conditions. This means that the cells are most likely primed and unable to undergo

translation, leading to a build-up of N-Cadherin RNA transcripts. The same idea could be seen in both *PAX3* and *TFAP2A* with build-up of transcripts due to low processing. However, an intriguing discrepancy arises when examining the pluripotency markers NANOG and *OCT4* within the 0.5 KPa and 0.75 KPa conditions. Particularly with NANOG, the expression closely resembles that of NBCs, suggesting the possible presence of an unprocessed transcript. One plausible explanation could involve the impact of low stiffness on transcript elimination, perhaps hindering a degradation complex. Still, a substantial difference between the 0.75 KPa and 0.5 KPa conditions hints at a potential threshold stiffness. This threshold might involve the inhibition of a mechanosensor crucial for transcript processing.

Contrastingly, *OCT4* seems less influenced by the overall stiffness shift, as all four stiffness conditions can be collectively considered under the umbrella term 'NCC.' A similar pattern emerges for *PAX3* and *TFAP2A*, hinting that these factors might remain unaffected by the shift in stiffness.

Shifting focus to neural crest specifiers, the uniformity in *SOX10* results (Figure 13D) suggests that stiffness might not significantly impact the *SOX10* transcript, potentially involving a distinct gene pathway. However, *TWIST1* shows clear distinctions between hard, soft conditions, and NBCs. The decrease in *TWIST1* expression aligns with the upregulations in E-Cadherin in the soft conditions. In the PCA data (Figure 13E), while stiffness data appears somewhat condensed, there's a possibility that low stiffness data points surround the concentrated cluster of stiff conditions. If confirmed with more data points, this would imply that cells in low stiffness conditions are distinct but closely related to both stiff

conditions and NBCs, representing a state of true cell neutrality. Considering the current results, it appears likely that partial EMT is occurring.

This line of thought leads to the concept of partial EMT, a phenomenon well-studied in cancer but less explored in early development. As of now partial EMT is primarily linked to cancer as opposed to wound healing and early development (Pastushenko et al., 2018), with certain cells displaying both epithelial and mesenchymal markers. Furthermore, many of the genes that were used in these experiments such as Twist and E-Cadherin, were not fully activated and in the process also leading to potential partial EMT. The idea of poised genes could also help explain the nature of the partial EMT, whereby some of the genes are activated whilst others are being held in a perpetual state and unable to progress. Additionally, poised genes are not entirely new concept as shown with cases in cancer(Bühler & Moazed, 2007), but this is a new idea that could arise for NCCs. Although much of this has been characterized in cancer, little is known about (Marjanovic, Weinberg, & Chaffer, 2013) this poised behaviour in early development. However, even in cancer, the exact nature of partial EMT and what causes this state is still ongoing.

Regardless of hypotheses, a few potential issues also arose throughout the process with one example being the idea of cell contamination. For example, as mentioned previously, although the reported number of cells differentiated to NCCs were high, they were never 100% and could be as low as 93%. Cells were also never FACS sorted, meaning that many of these could be another type of cell. Depending on what the cells may be, some of those other cell types could not only affect the mRNA that was used further down the line, but even the cells in culture. As a result, extracellular signals may be holding the differential

process back in a few of the cells while accelerating others. For example, in Figure 11, neural processes are clearly visible, indicating the possibility of cells being accelerated in differential state. This also led to the issue where cells were often shown to be more mesenchymal earlier than was reported by Kobayashi et al. As a result of this, morphologically it made more sense to study the cells earlier than the time proposed in the original paper. However, it is important to note that this only differed by a timeframe of around a day.

Similarly, if cells that are reseeded also have the possibility of already being mesenchymal, then any further differentiation that may occur may no longer be controlled, but stochastic. This can again be observed in Figure 11 with a few cells that are morphologically more neuronal than others. Again, this feeds into the potential inaccuracy that may be associated with these observed results. One potential solution to this would be to Fluorescence-activated cell sorting (FACS) to sort the cells to properly analyse their makeup and isolate the cells that are specifically of the desired type to enable a proper differential protocol. This is especially a problem with the later passages of hiPSC which can lead to issues of differentiation (Cantor et al., 2022).

Protein assays such as western blotting may also be useful in determining the extent of the poised state. Although with Figure 13, some of the RNA is shown to be at a high level, little is known about the protein that is produced from the RNA transcript. Being able to view and compare the differences between both the RNA levels and protein levels being produced may help determine what genes are being held in a 'poised' state and may be the target of the mechanosensing. Likewise, this will help narrow down some of the potential targets by also looking at other interactions that this protein may have.

Exploring the possibility of partial EMT would also require specific markers to identify and distinguish different EMT stages. However, the shared genes between EMT and NCC differentiation complicates this task. Recently, in collaboration with J. Hartmann, a postdoctoral researcher in the Mayor laboratory, analysed mouse neural crest single-cell RNA-seq data from Soldatov et al. (unpublished data). This analysis identified several potential gene candidates, offering a promising starting point for investigating the gene regulatory network associated with the observed phenotype. It's essential to note that these candidates were identified in mouse embryonic trunk neural crest cells, and differences in gene expression may exist between *in vivo* mouse trunk and *in vitro* human cranial neural crest cells. Nevertheless, this analysis provides a valuable foundation for further exploration.

To confirm the specific gene(s) responsible for the observed phenotype, additional experiments can be performed, such as gene knockdown or overexpression studies using techniques such as siRNA, CRISPR-Cas9, or gene editing tools. These experiments can help establish a cause-and-effect relationship between the candidate gene(s) and the observed phenotype. Further functional assays, such as *in vitro* or *in vivo* assays, can also be conducted to validate the role of the candidate gene(s) in the EMT process.
By identifying unique gene(s) associated with the observed phenotype, this research can contribute to a better understanding of the gene regulatory network controlling EMT in neural crest cells and provide insights into the underlying mechanisms driving the observed behaviour.

References:

Anderson, R. B., Stewart, A. L., & Young, H. M. (2006). Phenotypes of neural-crest-derived cells in vagal and sacral pathways. *Cell Tissue Res, 323*(1), 11-25. doi:10.1007/s00441-005-0047-6

Aragona, M., Dekoninck, S., Rulands, S., Lenglez, S., Mascré, G., Simons, B. D., & Blanpain, C. (2017). Defining stem cell dynamics and migration during wound healing in mouse skin epidermis. *Nat Commun, 8*, 14684. doi:10.1038/ncomms14684

Arnoux, V., Côme, C., Kusewitt, D. F., Hudson, L. G., & Savagner, P. (2005). Cutaneous wound reepithelialization. In *Rise and fall of epithelial phenotype*.

Balinsky, B. I. (1959). An electro microscopic investigation of the mechanisms of adhesion of the cells in a sea urchin blastula and gastrula. *Exp Cell Res, 16*(2), 429-433. doi:10.1016/0014-4827(59)90275-7

Barlow, P., Owen, D., & Graham, C. (1972). DNA synthesis in the preimplantation mouse embryo. *Development, 27*(2), 431-445.

Barriere, G., Fici, P., Gallerani, G., Fabbri, F., & Rigaud, M. (2015). Epithelial Mesenchymal Transition: a double-edged sword. *Clin Transl Med, 4*, 14. doi:10.1186/s40169-015-0055-4

Barriga, E. H., Franze, K., Charras, G., & Mayor, R. (2018). Tissue stiffening coordinates morphogenesis by triggering collective cell migration in vivo. *Nature, 554*(7693), 523-527. doi:10.1038/nature25742

Beningo, K. A., & Wang, Y.-l. (2002). Fc-receptor-mediated phagocytosis is regulated by mechanical properties of the target. *Journal of Cell Science, 115*(4), 849-856. doi:10.1242/jcs.115.4.849

Binnig, G., Quate, C. F., & Gerber, C. (1986). Atomic Force Microscope. *Physical Review Letters, 56*(9), 930-933. doi:10.1103/PhysRevLett.56.930

Bockman, D. E., & Kirby, M. L. (1984). Dependence of thymus development on derivatives of the neural crest. *Science, 223*(4635), 498-500. doi:10.1126/science.6606851

Bronner-Fraser, M. (1986). Analysis of the early stages of trunk neural crest migration in avian embryos using monoclonal antibody HNK-1. *Dev Biol, 115*(1), 44-55. doi:10.1016/0012-1606(86)90226-5

Bronner-Fraser, M. (1987). Perturbation of cranial neural crest migration by the HNK-1 antibody. *Dev Biol, 123*(2), 321-331. doi:10.1016/0012-1606(87)90390-3

Bronner-Fraser, M., & Fraser, S. E. (1988). Cell lineage analysis reveals multipotency of some avian neural crest cells. *Nature, 335*(6186), 161-164. doi:10.1038/335161a0

Bronner, M. E., & LeDouarin, N. M. (2012). Development and evolution of the neural crest: an overview. *Dev Biol, 366*(1), 2-9. doi:10.1016/j.ydbio.2011.12.042

Bühler, M., & Moazed, D. (2007). Transcription and RNAi in heterochromatic gene silencing. *Nature Structural & Molecular Biology, 14*(11), 1041-1048. doi:10.1038/nsmb1315

Butcher, D. T., Alliston, T., & Weaver, V. M. (2009). A tense situation: forcing tumour progression. *Nat Rev Cancer, 9*(2), 108-122. doi:10.1038/nrc2544

Câmara, D. R., Kastelic, J. P., & Thundathil, J. C. (2017). Role of the Na(+)/K(+)-ATPase ion pump in male reproduction and embryo development. *Reprod Fertil Dev, 29*(8), 1457-1467. doi:10.1071/rd16091

Canales Coutiño, B., & Mayor, R. (2021a). The mechanosensitive channel Piezo1 cooperates with semaphorins to control neural crest migration. *Development, 148*(23). doi:10.1242/dev.200001

Canales Coutiño, B., & Mayor, R. (2021b). Mechanosensitive ion channels in cell migration. *Cells & Development, 166*, 203683. doi:https://doi.org/10.1016/j.cdev.2021.203683

Cantor, E. L., Shen, F., Jiang, G., Tan, Z., Cunningham, G. M., Wu, X., . . . Schneider, B. P. (2022). Passage number affects differentiation of sensory neurons from human induced pluripotent stem cells. *Scientific Reports, 12*(1), 15869. doi:10.1038/s41598-022-19018-6

Carney, T. J., Dutton, K. A., Greenhill, E., Delfino-Machín, M., Dufourcq, P., Blader, P., & Kelsh, R. N. (2006). A direct role for Sox10 in specification of neural crest-derived sensory neurons. *Development, 133*(23), 4619-4630. doi:10.1242/dev.02668

Chambers, S. M., Fasano, C. A., Papapetrou, E. P., Tomishima, M., Sadelain, M., & Studer, L. (2009). Highly efficient neural conversion of human ES and iPS cells by dual inhibition of SMAD signaling. *Nat Biotechnol, 27*(3), 275-280. doi:10.1038/nbt.1529

Chhabra, S. N., & Booth, B. W. (2021). Asymmetric cell division of mammary stem cells. *Cell Division, 16*(1), 5. doi:10.1186/s13008-021-00073-w

Cook, D., Brown, D., Alexander, R., March, R., Morgan, P., Satterthwaite, G., & Pangalos, M. N. (2014). Lessons learned from the fate of AstraZeneca's drug pipeline: a five-dimensional framework. *Nat Rev Drug Discov, 13*(6), 419-431. doi:10.1038/nrd4309

Coulombe, P. A. (1997). Towards a molecular definition of keratinocyte activation after acute injury to stratified epithelia. *Biochem Biophys Res Commun, 236*(2), 231-238. doi:10.1006/bbrc.1997.6945

Cox, T. R., & Erler, J. T. (2011). Remodeling and homeostasis of the extracellular matrix: implications for fibrotic diseases and cancer. *Dis Model Mech, 4*(2), 165-178. doi:10.1242/dmm.004077

Du, W., Liu, X., Fan, G., Zhao, X., Sun, Y., Wang, T., . . . Li, X. (2014). From cell membrane to the nucleus: an emerging role of E-cadherin in gene transcriptional regulation. *J Cell Mol Med, 18*(9), 1712-1719. doi:10.1111/jcmm.12340

Dyce, J., George, M., Goodall, H., & Fleming, T. P. (1987). Do trophectoderm and inner cell mass cells in the mouse blastocyst maintain discrete lineages? *Development, 100*(4), 685-698.

Erickson, C. A., Duong, T. D., & Tosney, K. W. (1992). Descriptive and experimental analysis of the dispersion of neural crest cells along the dorsolateral path and their entry into ectoderm in the chick embryo. *Developmental Biology, 151*(1), 251-272. doi:https://doi.org/10.1016/0012-1606(92)90231-5

Faure, S., de Santa Barbara, P., Roberts, D. J., & Whitman, M. (2002). Endogenous patterns of BMP signaling during early chick development. *Dev Biol, 244*(1), 44-65. doi:10.1006/dbio.2002.0579

Förster, C. (2008). Tight junctions and the modulation of barrier function in disease. *Histochem Cell Biol, 130*(1), 55-70. doi:10.1007/s00418-008-0424-9

Frisch, S. M., & Francis, H. (1994). Disruption of epithelial cell-matrix interactions induces apoptosis. *J Cell Biol, 124*(4), 619-626. doi:10.1083/jcb.124.4.619

Graham, A., Begbie, J., & McGonnell, I. (2004). Significance of the cranial neural crest. *Developmental Dynamics, 229*(1), 5-13. doi:https://doi.org/10.1002/dvdy.10442

Gumbiner, B. M. (1996). Cell adhesion: the molecular basis of tissue architecture and morphogenesis. *Cell, 84*(3), 345-357. doi:10.1016/s0092-8674(00)81279-9

Haensel, D., & Dai, X. (2018). Epithelial-to-mesenchymal transition in cutaneous wound healing: Where we are and where we are heading. *Dev Dyn, 247*(3), 473-480. doi:10.1002/dvdy.24561

Handorf, A. M., Zhou, Y., Halanski, M. A., & Li, W. J. (2015). Tissue stiffness dictates development, homeostasis, and disease progression. *Organogenesis, 11*(1), 1-15. doi:10.1080/15476278.2015.1019687

Heng, B. C., Zhang, X., Aubel, D., Bai, Y., Li, X., Wei, Y., . . . Deng, X. (2020). Role of YAP/TAZ in Cell Lineage Fate Determination and Related Signaling Pathways. *Frontiers in Cell and Developmental Biology, 8*. doi:10.3389/fcell.2020.00735

Hudson, L. G., Newkirk, K. M., Chandler, H. L., Choi, C., Fossey, S. L., Parent, A. E., & Kusewitt, D. F. (2009). Cutaneous wound reepithelialization is compromised in mice lacking functional Slug (Snai2). *J Dermatol Sci, 56*(1), 19-26. doi:10.1016/j.jdermsci.2009.06.009

Hutchins, E. J., Kunttas, E., Piacentino, M. L., Howard, A. G. A. t., Bronner, M. E., & Uribe, R. A. (2018). Migration and

diversification of the vagal neural crest. *Dev Biol, 444 Suppl 1*(Suppl 1), S98-s109. doi:10.1016/j.ydbio.2018.07.004

Ito, M., Yang, Z., Andl, T., Cui, C., Kim, N., Millar, S. E., & Cotsarelis, G. (2007). Wnt-dependent de novo hair follicle regeneration in adult mouse skin after wounding. *Nature, 447*(7142), 316-320. doi:10.1038/nature05766

J.E. Coligan, B. M. D., H.L. Ploegh, D.W. Speicher, and P.T. Wingfield. (1995). *Electrophoresis, In Current Protocols in Protein Science*. New York: John Wiley and Sons.

Jang, K. J., Mehr, A. P., Hamilton, G. A., McPartlin, L. A., Chung, S., Suh, K. Y., & Ingber, D. E. (2013). Human kidney proximal tubule-on-a-chip for drug transport and nephrotoxicity assessment. *Integr Biol (Camb), 5*(9), 1119-1129. doi:10.1039/c3ib40049b

Jansen, K. A., Donato, D. M., Balcioglu, H. E., Schmidt, T., Danen, E. H., & Koenderink, G. H. (2015). A guide to mechanobiology: Where biology and physics meet. *Biochim Biophys Acta, 1853*(11 Pt B), 3043-3052. doi:10.1016/j.bbamcr.2015.05.007

Jiang, X., Gwye, Y., McKeown, S. J., Bronner-Fraser, M., Lutzko, C., & Lawlor, E. R. (2009). Isolation and characterization of neural crest stem cells derived from in vitro-differentiated human embryonic stem cells. *Stem Cells Dev, 18*(7), 1059-1070. doi:10.1089/scd.2008.0362

Jolliffe, I. (2014). Principal Component Analysis. In *Wiley StatsRef: Statistics Reference Online*.

Kandow, C. E., Georges, P. C., Janmey, P. A., & Beningo, K. A. (2007). Polyacrylamide hydrogels for cell mechanics: steps toward optimization and alternative uses. *Methods Cell Biol, 83*, 29-46. doi:10.1016/s0091-679x(07)83002-0

Kane, D. A., McFarland, K. N., & Warga, R. M. (2005). Mutations in half baked/E-cadherin block cell behaviors that are necessary for teleost epiboly. *Development, 132*(5), 1105-1116. doi:10.1242/dev.01668

Kim, T. J. (2021). Mechanobiology: A New Frontier in Biology. *Biology (Basel), 10*(7). doi:10.3390/biology10070570

Kisoda, S., Mouri, Y., Kitamura, N., Yamamoto, T., Miyoshi, K., & Kudo, Y. (2022). The role of partial-EMT in the progression of head and neck squamous cell carcinoma. *Journal of Oral Biosciences, 64*(2), 176-182. doi:https://doi.org/10.1016/j.job.2022.02.004

Knight, R. D., Nair, S., Nelson, S. S., Afshar, A., Javidan, Y., Geisler, R., . . . Schilling, T. F. (2003). lockjaw encodes a zebrafish tfap2a required for early neural crest development. *Development, 130*(23), 5755-5768. doi:10.1242/dev.00575

Kobayashi, G. S., Musso, C. M., Moreira, D. P., Pontillo-Guimarães, G., Hsia, G. S. P., Caires-Júnior, L. C., . . . Passos-Bueno, M. R. (2020). Recapitulation of Neural crest Specification and EMT via Induction from Neural Plate Border-like Cells. *Stem Cell Reports, 15*(3), 776-788. doi:10.1016/j.stemcr.2020.07.023

Krieg, M., Arboleda-Estudillo, Y., Puech, P. H., Käfer, J., Graner, F., Müller, D. J., & Heisenberg, C. P. (2008). Tensile forces govern germ-layer organization in zebrafish. *Nat Cell Biol, 10*(4), 429-436. doi:10.1038/ncb1705

Krieg, M., Fläschner, G., Alsteens, D., Gaub, B. M., Roos, W. H., Wuite, G. J., . . . Müller, D. J. (2019). Atomic force microscopy-based mechanobiology. *Nature Reviews Physics, 1*(1), 41-57.

Krishnan, R., Park, J. A., Seow, C. Y., Lee, P. V., & Stewart, A. G. (2016). Cellular Biomechanics in Drug Screening and Evaluation: Mechanopharmacology. *Trends Pharmacol Sci, 37*(2), 87-100. doi:10.1016/j.tips.2015.10.005

Kumai, J., Sasagawa, S., Horie, M., & Yui, Y. (2021). A Novel Method for Polyacrylamide Gel Preparation Using N-hydroxysuccinimide-acrylamide Ester to Study Cell-Extracellular Matrix Mechanical Interactions. *Frontiers in Materials, 8*. doi:10.3389/fmats.2021.637278

Kuo, B. R., & Erickson, C. A. (2011). Vagal neural crest cell migratory behavior: a transition between the cranial and trunk crest. *Dev Dyn, 240*(9), 2084-2100. doi:10.1002/dvdy.22715

Labouesse, C., Tan, B. X., Agley, C. C., Hofer, M., Winkel, A. K., Stirparo, G. G., . . . Chalut, K. J. (2021). StemBond hydrogels control the

mechanical microenvironment for pluripotent stem cells. *Nature Communications, 12*(1), 6132. doi:10.1038/s41467-021-26236-5

Lang, D., Chen, F., Milewski, R., Li, J., Lu, M. M., & Epstein, J. A. (2000). Pax3 is required for enteric ganglia formation and functions with Sox10 to modulate expression of c-ret. *J Clin Invest, 106*(8), 963-971. doi:10.1172/jci10828

Lawson, A., Anderson, H., & Schoenwolf, G. C. (2001). Cellular mechanisms of neural fold formation and morphogenesis in the chick embryo. *The Anatomical Record, 262*(2), 153-168. doi:https://doi.org/10.1002/1097-0185(20010201)262:2<153::AID-AR1021>3.0.CO;2-W

Leptin, M., & Affolter, M. (2004). Drosophila gastrulation: identification of a missing link. *Curr Biol, 14*(12), R480-482. doi:10.1016/j.cub.2004.06.016

Leung, A. W., Murdoch, B., Salem, A. F., Prasad, M. S., Gomez, G. A., & García-Castro, M. I. (2016). WNT/β-catenin signaling mediates human neural crest induction via a pre-neural border intermediate. *Development, 143*(3), 398-410. doi:10.1242/dev.130849

Lian, I., Kim, J., Okazawa, H., Zhao, J., Zhao, B., Yu, J., . . . Guan, K. L. (2010). The role of YAP transcription coactivator in regulating stem cell self-renewal and differentiation. *Genes Dev, 24*(11), 1106-1118. doi:10.1101/gad.1903310

Lim, C. T., Bershadsky, A., & Sheetz, M. P. (2010). Mechanobiology. *J R Soc Interface, 7 Suppl 3*(Suppl 3), S291-293. doi:10.1098/rsif.2010.0150.focus

Llames, S., García-Pérez, E., Meana, Á., Larcher, F., & del Río, M. (2015). Feeder Layer Cell Actions and Applications. *Tissue Eng Part B Rev, 21*(4), 345-353. doi:10.1089/ten.TEB.2014.0547

Marjanovic, N., Weinberg, R., & Chaffer, C. (2013). Poised with purpose: Cell plasticity enhances tumorigenicity. *Cell cycle (Georgetown, Tex.), 12*. doi:10.4161/cc.26075

Martin, A. C., & Goldstein, B. (2014). Apical constriction: themes and variations on a cellular mechanism driving morphogenesis. *Development, 141*(10), 1987-1998. doi:10.1242/dev.102228

Mikawa, T., Poh, A. M., Kelly, K. A., Ishii, Y., & Reese, D. E. (2004). Induction and patterning of the primitive streak, an organizing center of gastrulation in the amniote. *Dev Dyn, 229*(3), 422-432. doi:10.1002/dvdy.10458

Mikhailenko, S. V., Oguchi, Y., & Ishiwata, S. (2010). Insights into the mechanisms of myosin and kinesin molecular motors from the single-molecule unbinding force measurements. *J R Soc Interface, 7 Suppl 3*(Suppl 3), S295-306. doi:10.1098/rsif.2010.0107.focus

Montero-Balaguer, M., Lang, M. R., Sachdev, S. W., Knappmeyer, C., Stewart, R. A., De La Guardia, A., . . . Knapik, E. W. (2006). The mother superior mutation ablates foxd3 activity in neural crest progenitor cells and depletes neural crest derivatives in zebrafish. *Dev Dyn, 235*(12), 3199-3212. doi:10.1002/dvdy.20959

Moody, S. E., Perez, D., Pan, T. C., Sarkisian, C. J., Portocarrero, C. P., Sterner, C. J., . . . Chodosh, L. A. (2005). The transcriptional repressor Snail promotes mammary tumor recurrence. *Cancer Cell, 8*(3), 197-209. doi:10.1016/j.ccr.2005.07.009

Nakaya, Y., & Sheng, G. (2008). Epithelial to mesenchymal transition during gastrulation: An embryological view. *Development, Growth & Differentiation, 50*(9), 755-766. doi:https://doi.org/10.1111/j.1440-169X.2008.01070.x

Nakaya, Y., & Sheng, G. (2008). Epithelial to mesenchymal transition during gastrulation: an embryological view. *Dev Growth Differ, 50*(9), 755-766. doi:10.1111/j.1440-169X.2008.01070.x

Nani, D. A., Hsia, G. S. P., Passos-Bueno, M. R., & Kobayashi, G. S. (2022). Modeling Early Neural crest Development via Induction from hiPSC-Derived Neural Plate Border-like Cells. *Methods Mol Biol, 2549*, 281-298. doi:10.1007/7651_2021_454

Niu, Y., Sun, N., Li, C., Lei, Y., Huang, Z., Wu, J., . . . Tan, T. (2019). Dissecting primate early post-implantation development using long-term in vitro embryo culture. *Science, 366*(6467). doi:10.1126/science.aaw5754

O'Rahilly, R., & Müller, F. (1994). Neurulation in the normal human embryo. *Ciba Found Symp, 181*, 70-82; discussion 82-79. doi:10.1002/9780470514559.ch5

Oda, H., Tsukita, S., & Takeichi, M. (1998). Dynamic behavior of the cadherin-based cell-cell adhesion system during Drosophila gastrulation. *Dev Biol, 203*(2), 435-450. doi:10.1006/dbio.1998.9047

Odland, G., & Ross, R. (1968). Human wound repair. I. Epidermal regeneration. *J Cell Biol, 39*(1), 135-151. doi:10.1083/jcb.39.1.135

Özkale, B., Lou, J., Özelçi, E., Elosegui-Artola, A., Tringides, C. M., Mao, A. S., . . . Mooney, D. J. (2022). Actuated 3D microgels for single cell mechanobiology. *Lab on a Chip, 22*(10), 1962-1970. doi:10.1039/D2LC00203E

Pastushenko, I., Brisebarre, A., Sifrim, A., Fioramonti, M., Revenco, T., Boumahdi, S., . . . Blanpain, C. (2018). Identification of the tumour transition states occurring during EMT. *Nature, 556*(7702), 463-468. doi:10.1038/s41586-018-0040-3

Pelham, R. J., Jr., & Wang, Y. (1997). Cell locomotion and focal adhesions are regulated by substrate flexibility. *Proc Natl Acad Sci U S A, 94*(25), 13661-13665. doi:10.1073/pnas.94.25.13661

Pfaffl, M. W. (2001). A new mathematical model for relative quantification in real-time RT–PCR. *Nucleic Acids Research, 29*(9), e45-e45. doi:10.1093/nar/29.9.e45

Ramakers, C., Ruijter, J. M., Deprez, R. H. L., & Moorman, A. F. M. (2003). Assumption-free analysis of quantitative real-time polymerase chain reaction (PCR) data. *Neuroscience Letters, 339*(1), 62-66. doi:https://doi.org/10.1016/S0304-3940(02)01423-4

Raqeeb, A., Jiao, Y., Syyong, H. T., Paré, P. D., & Seow, C. Y. (2012). Regulatable stiffness in relaxed airway smooth muscle: a target for asthma treatment? *J Appl Physiol (1985), 112*(3), 337-346. doi:10.1152/japplphysiol.01036.2011

Rawles, M. E. (1948). Origin of melanophores and their role in development of color patterns in vertebrates. *Physiol Rev, 28*(4), 383-408. doi:10.1152/physrev.1948.28.4.383

Reedy, M. V., Faraco, C. D., & Erickson, C. A. (1998). Specification and migration of melanoblasts at the vagal level and in hyperpigmented Silkie chickens. *Dev Dyn, 213*(4), 476-485. doi:10.1002/(sici)1097-0177(199812)213:4<476::Aid-aja12>3.0.Co;2-r

Ribatti, D., Tamma, R., & Annese, T. (2020). Epithelial-Mesenchymal Transition in Cancer: A Historical Overview. *Transl Oncol, 13*(6), 100773. doi:10.1016/j.tranon.2020.100773

Rice, A. J., Cortes, E., Lachowski, D., Cheung, B. C. H., Karim, S. A., Morton, J. P., & del Río Hernández, A. (2017). Matrix stiffness induces epithelial–mesenchymal transition and promotes chemoresistance in pancreatic cancer cells. *Oncogenesis, 6*(7), e352-e352. doi:10.1038/oncsis.2017.54

Richards, M., Fong, C.-Y., Chan, W.-K., Wong, P.-C., & Bongso, A. (2002). Human feeders support prolonged undifferentiated growth of human inner cell masses and embryonic stem cells. *Nature Biotechnology, 20*(9), 933-936.

Rogers, C. D., Saxena, A., & Bronner, M. E. (2013). Sip1 mediates an E-cadherin-to-N-cadherin switch during cranial neural crest EMT. *J Cell Biol, 203*(5), 835-847. doi:10.1083/jcb.201305050

Saha, K., Kim, J., Irwin, E., Yoon, J., Momin, F., Trujillo, V., . . . Hayward, R. C. (2010). Surface Creasing Instability of Soft Polyacrylamide Cell Culture Substrates. *Biophysical Journal, 99*(12), L94-L96. doi:https://doi.org/10.1016/j.bpj.2010.09.045

Saitoh, M. (2018). Involvement of partial EMT in cancer progression. *The Journal of Biochemistry, 164*(4), 257-264. doi:10.1093/jb/mvy047

Savagner, P. (2007). *Rise and fall of epithelial phenotype: concepts of epithelial-mesenchymal transition*: Springer Science & Business Media.

Schor, S. L., & Schor, A. M. (1987). Foetal-to-adult transitions in fibroblast phenotype: their possible relevance to the

pathogenesis of cancer. *J Cell Sci Suppl, 8*, 165-180. doi:10.1242/jcs.1987.supplement_8.9

Schuliga, M., Javeed, A., Harris, T., Xia, Y., Qin, C., Wang, Z., . . . Stewart, A. G. (2013). Transforming growth factor-β-induced differentiation of airway smooth muscle cells is inhibited by fibroblast growth factor-2. *Am J Respir Cell Mol Biol, 48*(3), 346-353. doi:10.1165/rcmb.2012-0151OC

Shah, S. B., Skromne, I., Hume, C. R., Kessler, D. S., Lee, K. J., Stern, C. D., & Dodd, J. (1997). Misexpression of chick Vg1 in the marginal zone induces primitive streak formation. *Development, 124*(24), 5127-5138. doi:10.1242/dev.124.24.5127

Shamsan, G. A., & Odde, D. J. (2019). Emerging technologies in mechanotransduction research. *Current opinion in chemical biology, 53*, 125-130.

Shellard, A., & Mayor, R. (2021). Collective durotaxis along a self-generated stiffness gradient in vivo. *Nature, 600*(7890), 690-694. doi:10.1038/s41586-021-04210-x

Shibue, T., & Weinberg, R. A. (2017). EMT, CSCs, and drug resistance: the mechanistic link and clinical implications. *Nat Rev Clin Oncol, 14*(10), 611-629. doi:10.1038/nrclinonc.2017.44

Shih, I. M., Schnaar, R. L., Gearhart, J. D., & Kurman, R. J. (1997). Distribution of cells bearing the HNK-1 epitope in the human placenta. *Placenta, 18*(8), 667-674. doi:10.1016/s0143-4004(97)90008-4

Skloot, G., Permutt, S., & Togias, A. (1995). Airway hyperresponsiveness in asthma: a problem of limited smooth muscle relaxation with inspiration. *J Clin Invest, 96*(5), 2393-2403. doi:10.1172/jci118296

Skromne, I., & Stern, C. D. (2001). Interactions between Wnt and Vg1 signalling pathways initiate primitive streak formation in the chick embryo. *Development, 128*(15), 2915-2927. doi:10.1242/dev.128.15.2915

Soncin, F., Mohamet, L., Ritson, S., Hawkins, K., Bobola, N., Zeef, L., . . . Ward, C. M. (2011). E-cadherin acts as a regulator of transcripts associated with a wide range of cellular processes in mouse

embryonic stem cells. *PLoS One, 6*(7), e21463. doi:10.1371/journal.pone.0021463

Suresh, S., Spatz, J., Mills, J. P., Micoulet, A., Dao, M., Lim, C. T., . . . Seufferlein, T. (2005). Connections between single-cell biomechanics and human disease states: gastrointestinal cancer and malaria. *Acta Biomater, 1*(1), 15-30. doi:10.1016/j.actbio.2004.09.001

Takeichi, M. (1977). Functional correlation between cell adhesive properties and some cell surface proteins. *J Cell Biol, 75*(2 Pt 1), 464-474. doi:10.1083/jcb.75.2.464

Tam, P. P., & Loebel, D. A. (2007). Gene function in mouse embryogenesis: get set for gastrulation. *Nat Rev Genet, 8*(5), 368-381. doi:10.1038/nrg2084

Taneyhill, L. A. (2008). To adhere or not to adhere: the role of Cadherins in neural crest development. *Cell Adh Migr, 2*(4), 223-230. doi:10.4161/cam.2.4.6835

Theveneau, E., & Mayor, R. (2012). Neural crest delamination and migration: From epithelium-to-mesenchyme transition to collective cell migration. *Developmental Biology, 366*(1), 34-54. doi:https://doi.org/10.1016/j.ydbio.2011.12.041

Vestweber, D., & Kemler, R. (1985). Identification of a putative cell adhesion domain of uvomorulin. *Embo j, 4*(13a), 3393-3398. doi:10.1002/j.1460-2075.1985.tb04095.x

Wang, Y., Shi, J., Chai, K., Ying, X., & Zhou, B. P. (2013). The Role of Snail in EMT and Tumorigenesis. *Curr Cancer Drug Targets, 13*(9), 963-972. doi:10.2174/15680096113136660102

Warga, R. M., & Kimmel, C. B. (1990). Cell movements during epiboly and gastrulation in zebrafish. *Development, 108*(4), 569-580. doi:10.1242/dev.108.4.569

Xu, J., Lamouille, S., & Derynck, R. (2009). TGF-beta-induced epithelial to mesenchymal transition. *Cell Res, 19*(2), 156-172. doi:10.1038/cr.2009.5

Yan, C., Grimm, W. A., Garner, W. L., Qin, L., Travis, T., Tan, N., & Han, Y. P. (2010). Epithelial to mesenchymal transition in human skin wound healing is induced by tumor necrosis factor-alpha

through bone morphogenic protein-2. *Am J Pathol, 176*(5), 2247-2258. doi:10.2353/ajpath.2010.090048

Yang, J., Antin, P., Berx, G., Blanpain, C., Brabletz, T., Bronner, M., . . . On behalf of the, E. M. T. I. A. (2020). Guidelines and definitions for research on epithelial–mesenchymal transition. *Nature Reviews Molecular Cell Biology, 21*(6), 341-352. doi:10.1038/s41580-020-0237-9

Yu, M., Bardia, A., Wittner, B. S., Stott, S. L., Smas, M. E., Ting, D. T., . . . Maheswaran, S. (2013). Circulating breast tumor cells exhibit dynamic changes in epithelial and mesenchymal composition. *Science, 339*(6119), 580-584. doi:10.1126/science.1228522

Zeltner, N., Lafaille, F. G., Fattahi, F., & Studer, L. (2014). Feeder-free derivation of neural crest progenitor cells from human pluripotent stem cells. *J Vis Exp*(87). doi:10.3791/51609

Zhang, H. T., & Hiiragi, T. (2018). Symmetry Breaking in the Mammalian Embryo. *Annu Rev Cell Dev Biol, 34*, 405-426. doi:10.1146/annurev-cellbio-100617-062616